Zeynep ŞENEL CONTROL ALGORITHMS FOR FEEDBACK TRACKING IN THE SMALL POPULATIONS OF HODGKIN-HUXLEY NEURONS AGU 2018

CONTROL ALGORITHMS FOR FEEDBACK TRACKING IN THE SMALL POPULATIONS OF HODGKIN-HUXLEY NEURONS

A THESIS
SUBMITTED TO THE DEPARTMENT OF ELECTRICAL AND COMPUTER ENGINEERING AND THE GRADUATE SCHOOL OF ENGINEERING AND SCIENCE OF
ABDULLAH GUL UNIVERSITY
IN PARTIAL FULFILLMENT OF THE REQUIREMENTS
FOR THE DEGREE OF
MASTER OF SCIENCE

By
Zeynep ŞENEL
August 2018

CONTROL ALGORITHMS FOR FEEDBACK TRACKING IN THE SMALL POPULATION OF HODGIN-HUXLEY NEURONS

A THESIS
SUBMITTED TO THE DEPARTMENT OF ELECTRICAL AND COMPUTER ENGINEERING AND THE GRADUATE SCHOOL OF ENGINEERING AND SCIENCE OF
ABDULLAH GUL UNIVERSITY
IN PARTIAL FULFILLMENT OF THE REQUIREMENTS
FOR THE DEGREE OF
MASTER OF SCIENCE

By
Zeynep ŞENEL
August 2018

SCIENTIFIC ETHICS COMPLIANCE

I hereby declare that all information in this document has been obtained in accordance with academic rules and ethical conduct. I also declare that, as required by these rules and conduct, I have fully cited and referenced all materials and results that are not original to this work.

Name-Surname: Zeynep ŞENEL

REGULATORY COMPLIANCE

M.Sc. thesis titled Control Algorithms for Feedback Tracking in the Small Population of Hodgin-Huxley Neurons has been prepared in accordance with the Thesis Writing Guidelines of the Abdullah Gül University, Graduate School of Engineering & Science.

Prepared By	Advisor
Zeynep ŞENEL	Assoc. Prof. Dr. Sergey Borisenok

Head of the Electrical and Computer Engineering Program
Assoc. Prof. Vehbi Çağrı GÜNGÖR

ACCEPTANCE AND APPROVAL

M.Sc. thesis titled titled Control Algorithms for Feedback Tracking in the Small Population of Hodgin-Huxley Neurons and prepared by Zeynep ŞENEL has been accepted by the jury in the Electrical and Computer Engineering Graduate Program at Abdullah Gül University, Graduate School of Engineering & Science.

…….. /…….. / 2018

(Thesis Defense Exam Date)

JURY:

Advisor : Assoc. Prof. Dr. Sergey BORISENOK ……

Member : Prof. Dr. Recai KILIÇ……...

Member : Assoc. Prof. Kutay İÇÖZ ……..

APPROVAL:

The acceptance of this M.Sc. thesis has been approved by the decision of the Abdullah Gül University, Graduate School of Engineering & Science, Executive Board dated ….. /….. /2018 and numbered ……..……. .

…….. /…….. /2018

Graduate School Dean

Prof. Dr. İrfan ALAN

ABSTRACT

CONTROL ALGORITHMS FOR FEEDBACK TRACKING IN THE SMALL POPULATION OF HODGIN-HUXLEY NEURONS

Zeynep ŞENEL
MSc. in Electrical and Computer Engineering Department
Supervisor: Assoc. Prof. Dr. Sergey Borisenok

August 2018

The purpose of the thesis is to design powerful mathematical control algorithms for the tracking and modeling spiking and bursting behaviors of real biological neurons in 4-dimensional dynamical systems. For this aim, 4-dimensional Hodgkin-Huxley's (HH) nonlinear dynamical system including differential equations preferred. Because HH model represents a realistic mathematical model for the real neurons and it analytically accepted. Applied external current as a control signal initiate stimulating of the neuron cells in the neuronal networks serve while the membrane action potentials are outputs. We applied two different control methods; speed gradient (SG) of Fradkov's and target attractor (TA) of Kolesnikov's feedbacks for the modeling and controlling spiking and bursting regime that axon membrane potential created by the control signal in HH neuron clusters. These algorithms show high effectiveness and robustness in the managed HH dynamical neuron system.

This study provides generating arbitrary forms of single spikes, train of spikes and bursts for chosen cells in the various configurations of HH neuron clusters (linear chain and ring-type chain) with the control over a selected element of the network.

In this study, developed algorithms applied to epileptiform collective bursting in a small cluster of HH neurons for make suppression.

The scope of this thesis is to develop new control methods for mathematical modeling to control of real neurons and effectively can use in computational neuroscience and diagnosis or treatment of neural dysfunctions such as epileptiform or abnormal behavior in the HH neuron networks.

Keywords: Hodgkin-Huxley neuron, speed gradient method, target attractor feedback.

ÖZET

HODGIN-HUXLEY NÖRONLARININ KÜÇÜK POPULASYONUNDA GERİ BİLDİRİM İZLEME İÇİN KONTROL ALGORİTMALARI

Zeynep ŞENEL
Elektrik ve Bilgisayar Mühendisliği Ana Bilim Dalı, Yüksek Lisans Programı
Tez Yöneticisi: Doç. Dr. Sergey Borisenok
Ağustos 2018

Tezin amacı, 4 boyutlu dinamik sistemlerde gerçek biyolojik nöronların ani yükseliş ve fırlama davranışlarının izlenmesi ve modellenmesi için güçlü matematiksel kontrol algoritmaları tasarlamaktır. Bu amaçla 4 boyutlu Hodgkin-Huxley (HH) lineer olmayan diferansiyel denklemleri içeren dinamik sistem tercih edilir. Çünkü HH modeli gerçek nöronlar için gerçekçi bir matematik modeli temsil eder ve analitik olarak kabul edilmiştir. Bir kontrol sinyali olarak uygulanan dış akım, nöronal ağlardaki nöron hücrelerinin uyarılmasını başlatırken, membran eylem potansiyelleri çıkışlardır. HH nöron kümelerindeki kontrol sinyalinin yarattığı akson membran potansiyelinde ani yükseliş ve patlama rejiminin modellenmesi ve kontrol edilmesi için Fradkov'un hız gradyanı (SG) ve Kolesnikov'un hedef çekicisi (TA) geribildirimleri olmak üzere iki tane alternatif kontrol yöntemi kullanılmaktadır. Her iki algoritma da kontrollü HH dinamik nöron sisteminde yüksek verimlilik ve sağlamlık gösterir.

Bu çalışma, ağın seçilmiş bir unsuru üzerindeki kontrol ile HH nöron kümelerinin çeşitli konfigürasyonlarında (doğrusal zincir ve halka tipi zincir) rastgele tek ani yükseliş (spike), bir ani yükseliş dizisi (spike train) ve fırlama (burst) formlarının oluşturulmasını sağlamaktadır.

Bu çalışmada, geliştirilen algoritmalar küçük bir HH nöron kümesinde epileptik yapıdaki toplu fırlamalara baskılama yapmak için uygulanmıştır.

Bu tezin amacı, gerçek nöronların kontrolüne yönelik matematiksel modelleme için yeni kontrol yöntemlerinin geliştirilmesi ve hesaplamalı nörobilimde ve HH nöron ağlarında epileptik yapı veya anormal davranış gibi nöral fonksiyon bozukluklarının tanısı veya tedavisinde etkin bir şekilde kullanılabilmesidir.

Anahtar Kelimeler: Hodgkin-Huxley nöronu, hız gradyan metodu, hedef çekicisi geribeslemesi

Acknowledgements

I would like to express my sincerest gratitude to Dr. Sergei Borisenok offered abundant support and time to this thesis. His vast knowledge, guidance, patience, and motivation helped me to create this thesis.

I would like to thank TUBİTAK (project no. 116F049) for the supports of my scientific research and participation the conferences.

Table of Contents

1. INTRODUCTION ..... ….1

1.1 HUMAN BRAIN AND IMPORTANCE OF ITS STUDIES 1
1.2 NEURONS AND THEIR BASIC PROPERTIES. **HATA! YER İŞARETİ TANIMLANMAMIŞ.**
1.3 MODELLING AND CONTROL OF NEURONS 5
1.4 THE GOAL AND TOPIC OF THE RESEARCH 5

2. MATHEMATICAL MODELING OF REAL NEURONS ..... ….7

2.1 MATHEMATICAL MODELS FOR BIOLOGICAL NEURONS 7
2.2 HODGKIN-HUXLEY MODEL: PHENOMENOLOGICAL BACKGROUND AND ELECTRICAL CIRCUIT REPRESENTATION 10
2.3 DIFFERENTIAL EQUATIONS ABOUT HH MODEL 14
2.4 BASIC NONLINEAR DYNAMICAL PROPERTIES OF HH NEURON 17
2.5 CONCLUSION: CONTROLLABILITY OF HH MODEL 18

3. TRACKING ALGORITHMS FOR SINGLE HH NEURON ..... ….20

3.1 BASIC CONTROL ALGORITHMS FOR NEURON MODELS 20
3.2 SPEED GRADIENT ALGORITHM 23
3.3 TARGET ATTRACTOR ALGORITHM 24
3.4 NUMERICAL SIMULATIONS 26
3.5 TRACKING ERROR OF CONTROL 29
3.6 ENERGY POWER OF CONTROL 31
3.7 COMPARISON OF TWO METHODS AND CONCLUSIONS 32

4. TRACKING IN HH NEURON POPULATIONS ..... ….34

4.1 TRACKING IN LINEAR CHAINS 34
4.2 TRACKING IN LINEAR CHAINS WITH LOOPS 38
4.3 SUPPRESSING EPILEPTIFORM BEHAVIOR IN HH NEURONS VIA SG ALGORITHMS 41
4.4 CONCLUSIONS 47

5. CONCLUSIONS AND DISCUSSIONS ..... ….48

5.1 BASIC STATEMENTS OF THE THESIS 48
5.2 THE SET OF MAIN RESULTS 48
5.3 PERSPECTIVES OF THE RESEARCH 49
5.4 PARTICIPATION IN THE PROJECTS, CONFERENCES, PUBLICATIONS 49

BIBLIOGRAPHY ..... ….51

List of Figures

Figure 1.1: Schematic of the brain's parts 1
Figure 1.2: Schematic of a Neuron. Signals are moved through the axon via the action potential 3
Figure 1.3: Schematic of Action Potential 3
Figure 1.4: The gap called synapse that between two neuron 4
Figure 2.1: Circuit scheme of nerve model with the tunnel-diode from Nagumo et. al 8
Figure 2.2: The scheme of the cell membrane and distribution of ions and ionic channels by Hodgkin and Huxley 10
Figure 2.3: Diagram of a squid, showing the location of its giant nerve cells 11
Figure 2.4: Scheme of direct measurements of electrical potential in squid giant axon. (A) Capillary tube was filled with sea water has been carefully pushed down axon and serves as electrode to measure potential difference across membrane. (B) Membrane voltage *Vm* (in mV) during action potential. Time indicated by 500 Hz sine wave on oscilloscope screen 12
Figure 2.5: Marmont's space clamp with lateral guard electrodes: Diagram of squid axon and electrode arrangement for membrane controls. The axon passed along holes in the shaded insulating partitions. The central outside spiral electrode, for current and potential measurement, was between similar guard electrodes. The internal electrode, solid line, was inserted from the right to lie in the center of the axon 12
Figure 2.6: Voltage clamp technique for studying membrane currents of a squid axon 13
Figure 2.7: Electrical equivalent circuit suggested by Hodgkin and Huxley for a squid giant axon. The voltage-dependent conductances represented by the variable resistances 14
Figure 2.8: Diagrams explaining the gate dynamics 18
Figure 3.1: Tracking for the linear superposition of harmonics Eq. (3.13). The target potential *v*(t)* is denoted by red color, the actual action potential *v(t)* – by blue color. Left: speed gradient algorithm; Right: target attractor algorithm 26
Figure 3.2: Control parameter current as I(t) for the tracking goal Eq. (3.13). Left: speed gradient algorithm; Right: target attractor algorithm 27
Figure 3.3: Tracking for the burst-type pulse and the spike train Eq. (3.14). The target potential *v*(t)* is denoted by red color, the actual action potential *v(t)* – by blue color. Left: speed gradient algorithm; Right: target attractor algorithm 28
Figure 3.4: Error of tracking *e(t)* for speed gradient (green) and target attractor (black) algorithms. Left: the linear superposition of harmonics Eq. (3.13); Right: the bursting-and-spiking train Eq. (3.14) 29
Figure 3.5: The achievability of the control goal Eq. (3.2) in speed gradient algorithm for different control constants as gammas (γ). Horizontal axis: gamma constant in Eq. (3.4); Vertical axis: the stabilization level *v**. The color marks the quality of the stabilization (see the explanations above) 31
Figure 3.6: Power of tracking P(t) for speed gradient (pink) and target attractor (black) algorithms. Left: the linear superposition of harmonics Eq. (3.13); Right: the bursting-and-spiking train Eq. (3.14) 31

Figure 3.7: SG tracking of the target signal (red line) for different initial conditions; Vertical axes: the potantials in mV; Horizontal axes: time in ms 32
Figure 4.1: Basic model of pair of HH neurons 36
Figure 4.2: Tracking for the linear superposition of harmonics Eq. (3.13). The target potential $v^*(t)$ is denoted by red color, the actual action potential for first neuron v_1– by blue color. The actual action potential for second neuron v_2– by green color Left: speed gradient algorithm; Right: target attractor algorithm 37
Figure 4.3: Control parameter current as $I(t)$ for the tracking goal in linear chain Eq. (3.13). Left: speed gradient algorithm; Right: target attractor algorithm 38
Figure 4.4: Basic model of pair of HH neurons with loop 38
Figure 4.5: Tracking for the linear superposition of harmonics Eq. (3.13). The target potential $v^*(t)$ is denoted by red color, the actual action potential for first neuron v_1– by blue color. The actual action potential for second neuron v_2– by green color Left: speed gradient algorithm; Right: target attractor algorithm 40
Figure 4.6: Control parameter current as $I(t)$ for the tracking goal in close loop Eq. (3.13). Left: speed gradient algorithm; Right: target attractor algorithm 41
Figure 4.7: This color-enhanced brain scan of a person with epilepsy reveals that the focus of seizure activity is in the right frontal lobe, as shown by the large orange cluster at the top right of the image 42
Figure 4.8: Partial and Generalized Seizure 42
Figure 4.9: Basic model for an epileptiform suppression in the cluster of three Hodgin-Huxley neurons 43
Figure 4.10: Neurons membrane potentials vs. time (membrane potential for first neuron v_1– by blue color, for second neuron v_2– by green color, for third neuron v_3– by pink color) 46
Figure 4.11: Currents vs. time (I_{13}– by blue color, I_{23}– by green color, I_{31}– by pink color) 46

List of Tables

Table 2.1: Variables and coefficients according to Hodgkin-Huxley dynamic model...**16**

To My Family

It is nice to know you always support me

Chapter 1

Introduction

1.1 Human brain and importance of its studies

The brain is complicated organ as a part of the central nervous system in the human body. It is included in the skull as a soft tissue that has 1.4 kilograms weight. The brain responsible for processing all signals as consciously or unconsciously comes from the body, thought, feelings, memory and learning. Also, muscle activity, secretions of the glands, breathing, heart beating and regulation temperature are controlled by the brain.

The human brain builds from around 10^{11} neurons. The brains create a billion different connections continuously thorough our lives. The design and power of the connections are unstable so the brains don't like each other. Memories are stored to these changing connections thus our habits learned and personalities shaped.

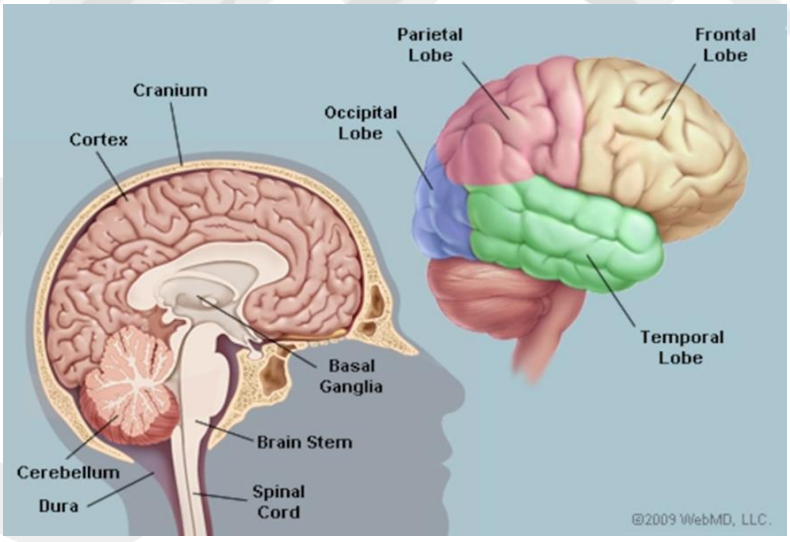

Figure 1.1: Schematic of the brain's parts [1].

The brain is constructed of many particular fields that work together:

- The **cortex** is the outer layer of brain cells. Thought and volitional movements start in this part.
- The **brain stem** connected with spinal cord. Its main functions such as sleeping and breathing are controlled there.

- The **basal ganglia** are a collection of structures in the middle of the brain. The basal ganglia organize information between multiple brain areas.
- The **cerebellum** is at the ground and the posterior of the brain. The role of cerebellum is balance and coordination.
- The **skull (cranium)** protects the brain from external strike.

The brain is also separated into a few lobes:

- The frontal lobes are in charge of motor function and judgment and problem solving.
- The parietal lobes organize body position, handwriting and sensation.
- The temporal lobes responsible for hearing and memory.
- The occipital lobes include the visual processing system of brain.

Thus, neuroscience is a flashing topic in the study for doctors, psychologists, and scientists. Their works continually progress but many questions are still unanswered. They attempt to achieve to learn exact structure of brain and how does it work. At the same time, they try to produce a solution to some brain disorders.

1.2 Neurons and their basic properties

Neurons are greatly specialized as electrically-excitable cells that are competent to make process and transmit neuronal signal. A neuron composes of dendrites, a soma (cell body) and axon.

Dendrites collect electrical signal from environment and to convey soma. The soma is covered by a semi-permeable cell membrane. This membrane has controlled the ions input and output from the cell. Presence of these ions differentiation causes the electrical charge in the neurons called that resting membrane potential. Action potential as an electrical response is produced by the neuron against the coming electrical signal. The action potential has propagated through the axon.

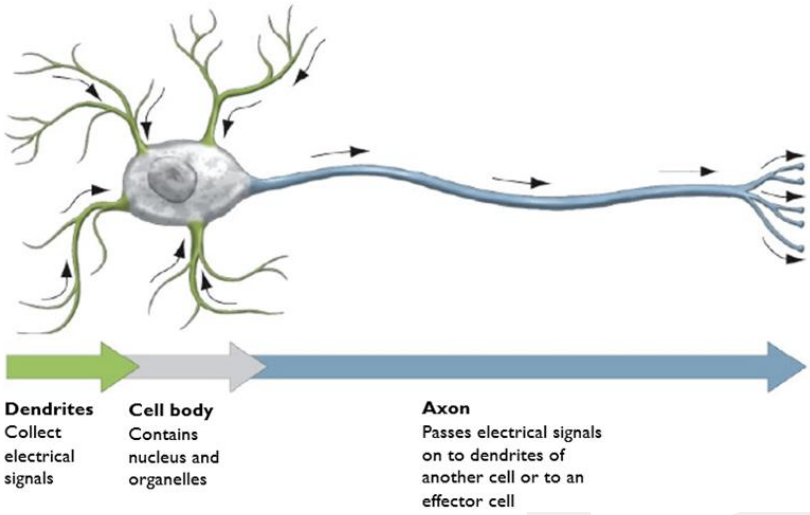

Figure 1.2: Schematic of a Neuron. Signals are moved through the axon via the action potential [2].

Action potentials have happened in the excitable cells covered that neurons, muscle cells, and endocrine cells. This signal provides that is propagated to transmission information through the axon. The formation of action potential is showed on Figure 1.3 with stepwise.

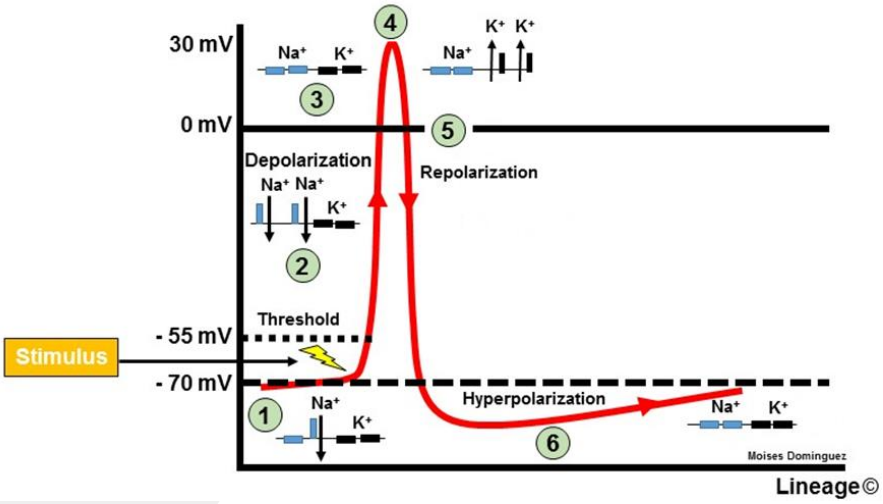

Figure 1.3: Schematic of Action Potential [3].

On the Figure 1.3 each step of process with numbered that expressed:

1. **Resting State:** At a first time, voltage-gated sodium and potassium channels are closed. More negatively charged membrane inside than outside.
2. **Depolarization:** When the stimulus reached to the threshold level, action potential begins to fire and sodium channels begin to open and sodium Na+ rush into the cell.

3. **Rising phase:** The inside of membrane is made more positive with respect to outside by more opened sodium channel and still closed potassium channel.
4. **Peak of the action potential:** The sodium channels have reached refractory stage and more sodium Na^+ isn't allowed to enter.
5. **Repolarization:** The most sodium channels become inactivated rapidly when most potassium channels open that permit to leave of potassium K+, thus inside of the membrane moves negative again.
6. **Hyperpolarization:** At this point, the sodium channels closed and some potassium channels open still so potassium K+ continue to leave the cell that become more negative than threshold to membrane..
1. **Resting State:** (repeated) When the potassium channels are closed, membrane returns resting again [4].

The signal is propagated through the axon. From there, signal transmits to the next neurons via synapses. Each neuron has hundreds or thousands connect with other neurons via small gaps called synapses. The neurotransmitters are released in the synapse to provide beginning of action potential for the next neuron. taken from a public source [4].

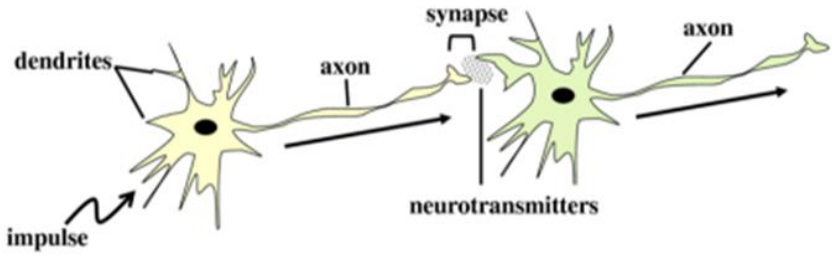

Figure 1.4: The gap called synapse that between two neuron [4].

Secretions of neurotransmitter demonstrate this is a chemical transmission at synapses. Most synapses contact with target neuron chemically. Chemical transmission is slower than electrical. According to the kind of synapse, an coming stimulus leads an increase in electrical potential as excitatory synapse or a decrease as inhibitory synapse [5].

1.3 Modeling and control of neurons

Mathematical models of spiking neurons cover entire fields of modern mathematics. They are usually written in the form of ordinary differential equations with multidimensional formulations. The neuronal networks with spike behaviors have a substantial role in different applications of computational neuroscience [6] [7] and pattern identification [8]. Biological neurons exhibit a variety of complex dynamic behaviors involving differences between steady and spike states at different time scales [9] [10] [11]. Differences in the steady and spike systems in real neurons cause bursting features to occur and construct the basis for the flow of information by providing intercellular communication.

Such irregular behavioral mechanisms are also due to the networks between the neurons as well as the internal structure of them. In the event of a bursting, one or a series of spikes or spikes of train are produced on the axon which an external electric current (signal) coming from the neighboring cell to dendrite and stimulated by the data processing process of the cell of soma itself. The bursting has generally a chaotic dynamic character [12], [13] and is a semi-periodic process.

Transitions between bursting and spiking events have been studied experimentally for different neurons such as pyloric dilator [14], lateral pyloric [15], midbrain dopaminergic [16], striatal and pallidumal [17], pyramidal neurons [18] [19]. Methods also include optogenetic regulation [20] and carbon nanotube and single nerve cell interface [21] [22] as well as electrical micro stimulus [23]. But, such practical approaches require the development of an effective theoretical control algorithm that will design the targeted dynamic state of the spiking neuron.

1.4 The goal and topic of the research

The topic of proposed study in this thesis is to improve the control algorithm that are produce the desired spiking and bursting states of neural networks.

The thesis is illustrated through the following outputs:

- **Mathematical Model:** The 4-dimensional Hodgkin-Huxley derivative system, which shows all the basic features (the design of the spiking under the influence of the external current and to put the existence of the threshold value for this situation) and dynamic states (the interval between

the spiking and the steady state, to obtain of the spiking and the chaotic bursting) of the system, is chosen between different mathematical models on neurons obtained from experimental data on real cells.

- **Control algorithms for tracking:** The proven "Speed Gradient" (SG) and "Target Attractor" (Synergetic) feedback methods that effectively demonstrate the dynamic modeling of many physical and biological phenomena, have been chosen as two different approaches for solving the problem. In the phase space, Speed Gradient (SG) is a system control algorithm that gently evolves the expected spiking and bursting situation to desired value and Target Attractor (TA) algorithm that forces the system to go to desired value exponentially. Implementation of two different algorithms will provide flexibility in reducing the risks that can affect the success of the thesis.

  The two algorithms (SG and TA) used in the study that are stable under poor stochastic perturbations [24] [25], it should be reminded that the noise under feedback control and the perturbed HH neurons are another research topic.
- **Purpose of control:** As normally or chaotically production of artificial bursting and spiking signals that will not require the reproduction of the internal dynamics of the HH neuron model.
- **Establishment of the neural network architecture:** The simplest networks (straight line, triangle and quadrilateral) that can be installed for one or several neuron clusters offer the opportunity to examine the effects of communication of the HH pairs over different network structures on spiking and bursting signals.

Thus, the purpose of the study is not only synchronous pulses created within the framework of its own dynamics of the HH neuron, also, it is aimed to direct the arbitrarily designed target dynamic state in the Hodgkin-Huxley system with the dynamic properties of one or several neurons in the cluster to provide the targeted spiking and bursting characteristics of the single neuron. Among the mentioned algorithms, SG and TA have been selected because they are the most suitable for this purpose and should be available for possible changes such as adding noise and time delay in the future.

Chapter 2
Mathematical Modeling of Real Neurons

2.1 Mathematical models for biological neurons

The countless coupling neurons provide transferring of data in the biological nervous network. Neurons have handled all this process by the action potentials. On the basis of the important electrical activities as action potentials, various mathematical models [26] [27] have been produced to contribute expressing of real neuron behavior theoretically. Here, we have chosen to mention most commonly used mathematical models for real neurons.

2-dimensional Planar Hybrid Spiking model (2-D HS model) which 2 parameters constructed to describes the action potential and all ion gates. It was created by reducing HH model in the phase space plane. The planar HS model has one voltage and one gating variable for make exampling the behavior of conductance based models with high-dimensional [28]. That is, the planar HS model is easy and useful model that needs to one variable for making the action potential. But there is a disadvantage 2-dimensional model does not include intermittent regime [29] and damping state [30] in continuous time.

FitzHugh-Nagumo (FN) model [31] [32], as redefined by Izhikevich [33] [34] and others [35] [36] [37] are the most famous neuron models.

The dimensionless action potential *v* and the dimensionless constant *w* represent the ions tunneled through ion gates. The fastest output of the system is the start and end of the sudden rise. The electric current *I*, who stimulates this situation, plays the role of the control signal. The function *f(v)* is usually polynomial. In such a case, the equation must be at least a third-order equation to ensure the presence condition of the unique limit cycle described in the Poincaré-Bendixson theorem [38]. This cycle is responsible for switching between stagnant and sudden ascent conditions. A special case of the HS family is that according to the FitzHugh-Nagumo model [31] [32], a is a constant greater than zero;

$$f(v) = v(1-v)(v-a) \tag{2.1}$$

The FitzHugh-Nagumo model is [31] [32] representing to reduce the HH model of such spike production at squid giant axons from a 4-dimensional to a 2-dimensional. FHN model mimic the rich dynamical behavior of many cell types. Here, *v* is the neuron membrane potential shows slow dynamics, *w* is a recovery variable correspond to fast dynamics close to hyperpolarizing action potential, *I* is the stimulus current applied externally. The model can be described in various forms but is often written in the theoretical form;

$$\frac{dv}{dt} = f(v) - w + I \; ; \qquad \textbf{(2.2)}$$

$$\frac{dw}{dt} = a(bv - cw) \; .$$

where *f(v)* is a polynomial of third degree, *a* and ,*b* ,*c* and are constant parameters [39]. The equations represent the behavior of a neuron, the parameters *a, b* and *c* are set in a certain range [32] [40] [41], and the conventional values are *a*=0.7, *b*=0.8, *c*=3 [42]. When the *a*=*b*=0 FHN model return to the nonlinear Van der Pol oscillator [31] by reduced.

This system is also called as the "Bonhoeffer-van der Pol (BVP) oscillator", derived from van der Pol equation suggested by FitzHugh [40] and the equivalent electrical circuit with tunnel diode by Nagumo [32].

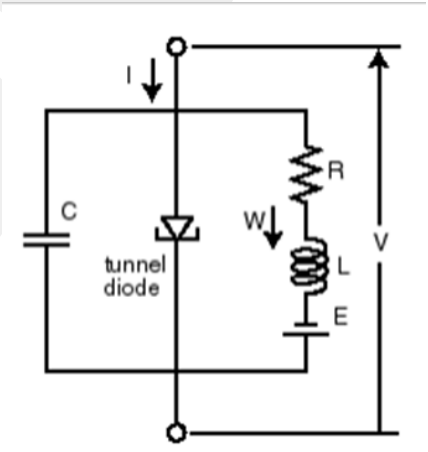

Figure 2.1: Circuit scheme of nerve model with the tunnel-diode from [32].

Many theoretical analyses revealed that FHN model is described dynamical nature of bursting, it including chaos, bifurcations, circuit design, filtering, noise effect and coupling, etc. [28] [43].

Another reduced version of the HH model is a 3D Hindmarsh-Rose (HR) model has the dimensionless *v(t)* potential and two variables (*wf(t)* and *ws(t)*) corresponding to fast ion channels (sodium and potassium) and slow channel [44]:

$$\begin{aligned} \frac{dv}{dt} &= -av^3 + bv^2 + w_f + I \ ; \\ \frac{dw_f}{dt} &= c - d \cdot v^2 - w_f \ ; \\ \frac{dw_s}{dt} &= r\left[s(v - v_0) - w_s\right]. \end{aligned} \qquad \textbf{(2.3)}$$

The set of larger than zero constants *a, b, c, d* is used to identify fast ion channels and *r* is used to identify slow ion channels. The other two variables are empirical and are usually $s = 4$ and $v_0 = -1.6$.

An important extension of the planar model is also in the complex domain. The modeling of natural objects in this way indicates that the "quantum neuron" has its non-classical properties (first [45] mentioned) or synaptic quantum tunneling neurotransmitters [46] due to the tunneling of ion gates.

Models such as cubic-based quantum spiking modeling for neurons [47] are also available. The most famous notations in this class are the Josephson junction (JJ) [48] [49], which shows advanced dynamics for the connected neuron pair [50]. Quantum body control has its own characteristics [51]. Detailed research on the JJ neuron model is within the scope of future studies following the current study. In this case, it will be possible to make detailed comparisons of spiking and bursting algorithm for the neurons at the classical and quantum level.

In all of the models discussed above, the current *I* stimulates the membrane as an external control parameter. Typically this control current is of the fixed or simple step function type.

2.2 Hodgkin-Huxley model: Phenomenological background and electrical circuit representation

The modeling neural excitability and understanding behavior of neurons have been essentially affected by the cornerstone study of Hodgkin and Huxley. They have a series of five Journal of physiology articles [26] [52] [53] [54] [55] published in 1952 these researcher (together with as co-author and their collaborator Bernard Katz,) revealed the important features of the ionic conductances of the nerve action potential and constructed the nonlinear ordinary differential equations that show the generation and propagation of action potentials along an axon. Hodgkin and Huxley have awarded to the 1963 Nobel Prize in Physiology and Medicine (they shared with John Eccles) by this successful clarification. Hodgkin and Huxley applied new experimental techniques for defining membrane features in their first four paper that proving experimental achievement while their last paper in the series brought theoretically our modern perspective of neural excitability [56]. Thereby, Hodgkin and Huxley model was an ideal neuron model system give chance to apply new techniques for tracking the problem comprehensively.

The neurons' cytoplasm has a low-resistance covered by membrane has a high-resistance. As seen in Fig. 2.2, inside and outside of cell membrane have different ionic concentrations of solutions. The inside has higher concentration of potassium than outside and the outside has higher concentration of sodium than inside. The membrane defined by an electrical capacitance.

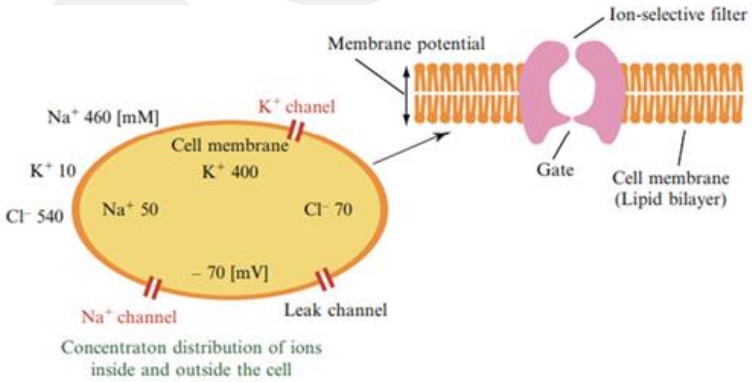

Fig. 2.2: The scheme of the cell membrane and distribution of ions and ionic channels by Hodgkin and Huxley [57].

Additionally, there was a difference of electrical potential caused to membrane potential between the outside and the inside of the cell. The membrane potential was not enable to measure directly until 1940. These indirect measurements were made only with extracellular electrodes get about limited information of membrane potential. But, Hodgkin and Curtis accomplished to direct measurement of membrane potential (*Vm*) thorough the squid giant axon via a glass micropipette (Fig. 2.4A). The squid giant axon ultimately has served to their works. It allows comfortable preparation for the experiments with an extraordinarily large axon has 1mm in diameter, 100 to 1000 times larger than mammalian axons, and minimal conductance[58] [59].

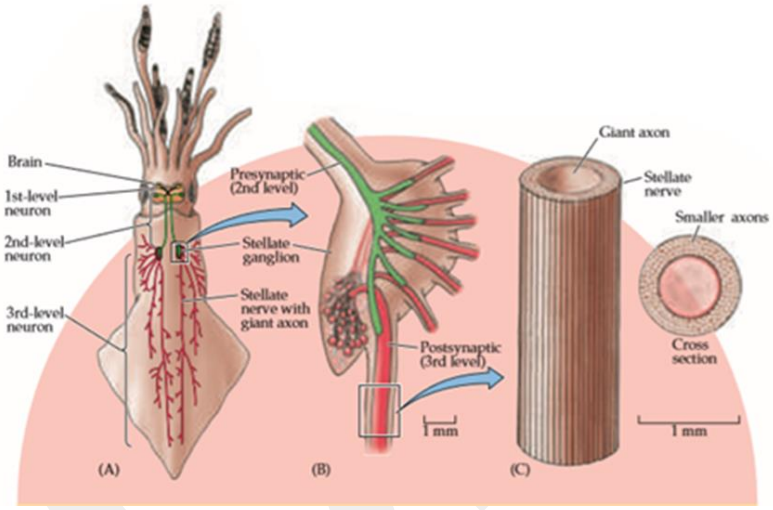

Figure 2.3: Diagram of a squid, showing the location of its giant nerve cells [60].

Finally, both Hodgkin and Curtis other collaborators [61] [62] have been successful and they noticed both the membrane potential (*Vm*) goes temporarily toward zero [63], also there was a considerable overshoot (Fig. 2.4B).

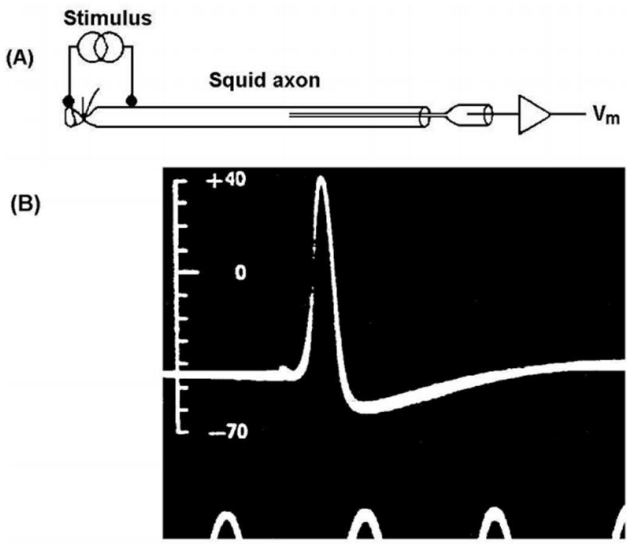

Figure 2.4: Scheme of direct measurements of electrical potential in squid giant axon. **(A)** Capillary tube was filled with sea water has been carefully pushed down axon and serves as electrode to measure potential difference across membrane. **(B)** Membrane voltage *Vm* (in mV) during action potential. Time indicated by 500 Hz sine wave on oscilloscope screen [59].

During the action potential, the proposed essential experimental techniques that are: the space clamp and the voltage clamp techniques to analyze of the membrane alteration.

- **Space Clamp Technique**

Marmont and Cole worked on the space clamp technique to continue a uniform spatial distribution of membrane voltage (*Vm*) of the cell by inserting a long thin stimulation electrode into the axon and the other metal cylindrical electrode outside the axon [64] [65]. Thus the potential can only change with diameter of axis and radial currents. As a result, all membrane elements are in a harmony. [59] [66] [67].

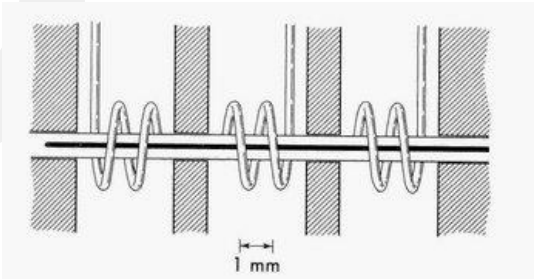

Figure 2.5: Marmont's space clamp with lateral guard electrodes: Diagram of squid axon and electrode arrangement for membrane controls. The axon passed along holes in the shaded insulating partitions. The central outside spiral electrode, for current and potential measurement, was between similar guard electrodes. The internal electrode, solid line, was inserted from the right to lie in the center of the axon [67].

- **Voltage Clamp Technique**

Kenneth Cole and partners also developed the voltage clamp technique to set holding membrane potential at any desired level in the 1940s. They using two couples of electrodes that one provided to measurement of the voltage with a microelectrode placed inside the cell against the membrane and the other is provided to insert current to clamp the desired voltage. Thus, this technique can demonstrate how membrane potential effects ionic current flow across the membrane [59] [60] [68].

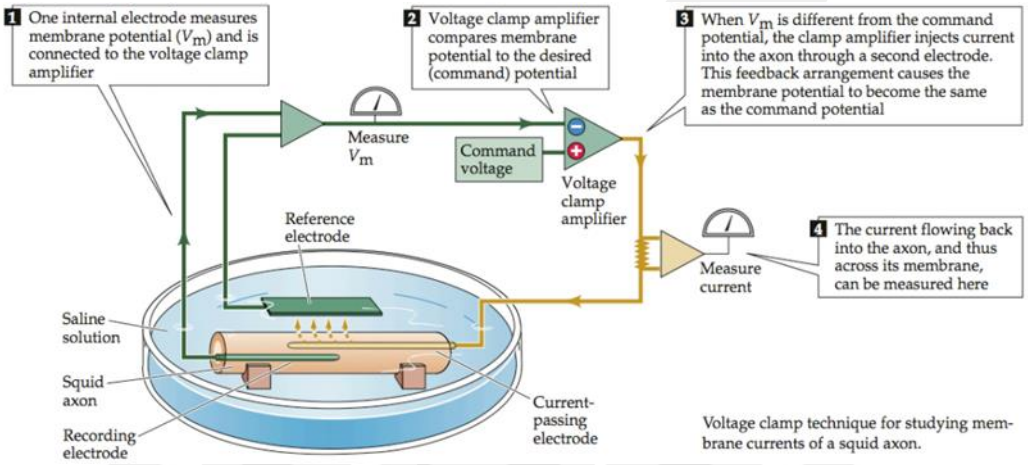

Figure 2.6: Voltage clamp technique for studying membrane currents of a squid axon [60].

Hodgkin and Huxley determined various individual ionic currents using the above techniques [66].

Electrical Equivalent Circuit

Basic idea of the HH model is to define nerve membrane with the electrical features as an equivalent circuit form seen from in Fig. 2.7. The equivalent circuit of HH model is including important three ionic currents as a sodium current I_{Na}, a potassium current I_K, and remaining ionic currents accumulated in a small leakage current I_L which is mainly moved by chloride ions.

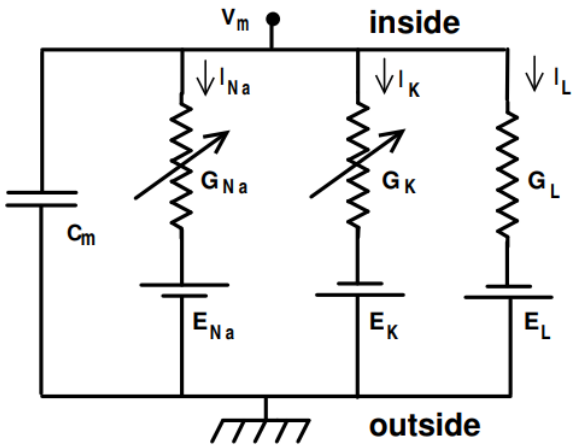

Figure 2.7: Electrical equivalent circuit suggested by Hodgkin and Huxley for a squid giant axon. The voltage-dependent conductances represented by the variable resistances.[55].

where *Cm* is a capacitor represent to the capacitive property of the cell membrane, *Vm* denotes the membrane potential, sum of I_{Na}, I_K, and I_L represents the net ionic current that flows against the membrane, and *I* is an applied current externally.

The behavior of the electrical circuit was defined by a set of differential equation [59] shown in next sub-chapter (2.3).

2.3 Differential equations about HH model

Hodgkin and Huxley was produced a suitable model for a single neuron in 1952 and received the 1963 Nobel Prize for Medicine. The model contains four independent variables: one of them represents the action potential and three parameters stand for the probabilities of the opening and closing membrane ion gates. In the 4-dimensional case, the HH model, including steady and damping of spiking, has been redefined to gate variables in the literature [69] and showed the variation of neuron dynamics in normal and chaotic states [70] [71] [72] [73] [74].

The set of differential equations given by the HH model [26]:

$$C_M \cdot \frac{dv}{dt} = -g_{Na} m^3 h \cdot (v - E_{Na}) - g_K n^4 \cdot (v - E_K) - g_{Cl} \cdot (v - E_{Cl}) + I \; ; \qquad \textbf{(2.4a)}$$

$$\begin{aligned} \frac{dm}{dt} &= \alpha_m(v) \cdot (1-m) - \beta_m(v) \cdot m \; ; \\ \frac{dn}{dt} &= \alpha_n(v) \cdot (1-n) - \beta_n(v) \cdot n \; ; \\ \frac{dh}{dt} &= \alpha_h(v) \cdot (1-h) - \beta_h(v) \cdot h \; ; \end{aligned} \qquad \textbf{(2.4b)}$$

$$I_{Na} = g_{Na} m^3 h \cdot (v - E_{Na}); I_K = g_K n^4 \cdot (v - E_K); I_L = g_{Cl} \cdot (v - E_{Cl}). \qquad \textbf{(2.4c)}$$

Here the membrane potential represented by *v(t)* while *m(t), n(t), h(t)* are stand for the membrane gate variables, and *I(t)* serves as the control signal is demonstrated by the total amount of currents coming to the neuron that are externally and synaptically. Here $\alpha m,n,h$ and $\beta m,n,h$ are fenomenologically created convenient rate positive constant link to the gate probabilities, they are written as follow:

$$\alpha_m(v) = \frac{0.1 \cdot (25 - v)}{\exp\left\{\frac{25 - v}{10}\right\} - 1} \; ; \; \beta_m(v) = 4 \cdot \exp\left\{-\frac{v}{18}\right\} ;$$

$$\alpha_n(v) = \frac{0.01 \cdot (10 - v)}{\exp\left\{\frac{10 - v}{10}\right\} - 1} \; ; \; \beta_n(v) = 0.125 \cdot \exp\left\{-\frac{v}{80}\right\} ; \qquad \textbf{(2.5)}$$

$$\alpha_h(v) = 0.07 \cdot \exp\left\{-\frac{v}{20}\right\} \; ; \; \beta_h(v) = \frac{1}{\exp\left\{\frac{30 - v}{10}\right\} + 1} \; .$$

The set of constants in Eq. (2.4) includes the potentials E_{Na} (equilibrium potential at which the net flow of Na ions is zero), E_K (equilibrium potential at which the net flow of K ions is zero), E_{Cl} (equilibrium potential at which leakage is zero) in mV, the membrane capacitance C_M and the conductivities g_{Na} (sodium channel conductivity), g_K (potassium channel conductivity), g_{Cl} (leakage channel conductivity) in mS/cm^2:

$$\begin{aligned} g_{Na} &= 120; \; E_{Na} = 115; \\ g_K &= 36; \quad E_K = -12; \\ g_{Cl} &= 0.3; \; E_{Cl} = 10.36, \end{aligned} \tag{2.6}$$

Descriptions of variables and constants are given in Table 2.1.

VARIABLES	
$v(t)$	Membran potential; ***dynamic variable***
$m(t)$, $n(t)$, $h(t)$	Membran gate variables; ***dynamic variables***
$I(t)$	Total amount of currents coming to the neuron that are externally and synaptically; ***Control signal***
CONSTANTS	
E_{Na}	When the net current of sodium (Na) ions is zero, the equilibrium potential
E_K	When the net current of potassium (K) ions is zero, the equilibrium potential
E_{Cl}	When the leakage current is zero, the equilibrium potential
C_M	Membrane resistance
g_{Na}	Sodium channel conductance
g_K	Potassium channel conductance
g_{Cl}	Leakage channel conductance
$\alpha, \beta_{m, n, h}$	Suitable coefficients found empirically

Table 2.1: Variables and coefficients according to Hodgkin-Huxley dynamic model.

Dynamics of Hodgkin-Huxley neurons have diversity of regular and chaotic regimes [70] [71] [72] [74]. It covers the resting-and-spiking intermittency because of it is 4-dimentional.

Some properties of the HH model Eqs. (2.4) ; (2.6) that reflects real behaviors of biological neurons in a realistic way are given below:

a) Without any external current I as a stimulation, neurons can't generation to spike;

b) I should be at least a threshold level [75], for example HH neuron can produce spike when applied the stimulation even with a constant current, but the current have to be larger than a possible minimum threshold level.

When the control algorithms applied to the single control parameter *I(t)* gives opportunity to regeneration the different dynamical regimes in the model Eqs. (2.4) ; (2.6).

But in the HH neuron network, it is possible to produce spiking conditions in common with an external signal below the threshold [76] [77].

2.4 Basic nonlinear dynamical properties of HH neuron

The Hodgkin–Huxley equations [26] obtained from experiments of a squid giant axon. These simply dynamical equations come from the electric circuit demonstrated in Fig. 2.7 and are defined in Eqs. (2.4-2.6). V (mV) is the membrane potential. The equation Eq. (2.4a) clearly indicates the Kirchhoff's law. I_{Na} and I_K currents flow through Na^+ and K^+ channels, respectively. The current I_L is the leak current that represents all residue currents, mostly comes from Cl^- ions, along a cell membrane except for Na^+ and K^+ currents. I_{Na} is expressed by $g_{Na}m^3h.(v\text{-}E_{Na})$ which comes from (Conductance × Voltage) that is Ohm's law. The voltage E_{Na} is denoted by the Nernst potential or the resting potential or equilibrium potential of Na^+ ion. It shows the equilibrium potential when the net current of sodium (Na) ions is zero. Also E_K and E_L represent to the equilibrium potential when the net current of sodium (K) ions and leakage is zero respectively. When the membrane is permeable with different degrees to more than one ionic species, to calculate the steady state potential used the Nernst Equation that produced by D.Goldman. but it named the Goldman-Hodgkin-Katz equation has applied widely. Where the reference rest potential is given:

$$
\begin{aligned}
v_{\text{rest}} &= 58\log\left(\frac{P_K\cdot K_{\text{ext}} + P_{Na}\cdot Na_{\text{ext}} + P_{Cl}\cdot Cl_{ext}}{P_K\cdot K_{\text{int}} + P_{Na}\cdot Na_{\text{int}} + P_{Cl}\cdot Cl_{\text{int}}}\right);\\
K_{\text{ext}} &= 20;\ K_{\text{int}} = 400;\\
Na_{\text{ext}} &= 440;\ Na_{\text{int}} = 50;\\
Cl_{\text{ext}} &= 560;\ Cl_{\text{int}} = 150;\\
P_K &= 1;\ P_{Na} = 3;\ P_{Cl} = 0.45.
\end{aligned}
\qquad \textbf{(2.7)}
$$

For the K^+ current I_K, the description of n^4 represent the temporal change of K^+ channel conductance. The gate variables that dimensionless term *m*, *n* and *h* take a value between zero and one.

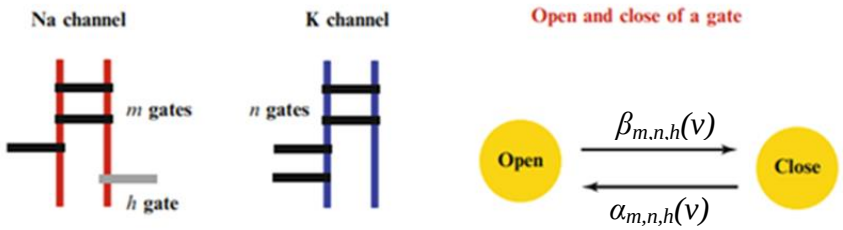

Fig. 2.8: Diagrams explaining the gate dynamics [57].

On the left side of Fig. 2.8, it is assumed that Na^+ channel has three *m*-gates and single *h*-gate while K^+ channel has four n-gates. In the HH model, it is also assumed that the probabilities of gates open state defined by variables *m*, *n* and *h*. The rate constants defined by Eq. (2.4b) adjust the dynamic of opening and closing process of gates. As seen from the right side of Fig. 2.8, as one of the rate constant is $\alpha_m(v)$ provides close to switch open state, while another rate constant is $\beta_m(v)$ serve as a switch from open to close state. Actually these rate constants $\alpha_m(v)$ and $\beta_m(v)$ are not constant, they are functions based on membrane potential (v) described by Eq. (2.5). Activation variables is m and inactivation variables is n for Na^+ ionic channel while n the activation variable for K^+ channel. Because of this reason m and n are the increasing functions of v whereas h the decreasing one. I (μA cm-2) is applied current as a constant externally to a neuron [57].

2.5 Conclusion: Controllability of HH model

There are crucial reasons in we chose the 4-dimensional Hodgkin-Huxley ordinary differential system among the diversity of mathematical models for biological neurons. Firstly, HH model reflects behavior of real cells because it has been phenomenologically derived from the experiments with real biological excitability cells also indicates all basic features (spiking under external electrical current stimulation, existence of a threshold for spiking regime) and dynamical regimes (intermittency of spiking and resting, generation of spike trains, chaotic bursting) of a biological neuron.

The HH model has a free control parameter, the external signal I, and it is well-designed for the application of different control algorithms, that will be discussed in Chapter 3.1, especially in speed gradient (SG) and target attractor (TA) feedback forms for 4-dimensional Hodgkin-Huxley neurons and their clusters. The study of basic cluster configurations for HH neuronal network with controlled elements provides an effective tool for driving collective neuron bursting and serves as the most natural computational neuroscience model for real neuronal networks.

Chapter 3

Tracking Algorithms for Single HH Neuron

3.1 Basic control algorithms for neuron models

Biological dynamical systems have mostly multidimensional, nonlinear, hierarchical, and noisy features that demand; fixed-point control (maintenance of posture, homeostatic control), control of rhythmic movements (locomotion, respiratory control), control of rhythmic processes (circadian activation, oscillatory neural activity). Commonly control theory in all areas have potential application to biological neural and motor systems, covering feedback control; prediction and control of nonlinear systems; geometric control; optimization-based control; stability analysis; model description and parameter prediction; estimation model control; detectability and controllability in the networks; and stochastic control. Simultaneously, control theory is stretched by the biological control problems with new directions. It often deals with negative feedback control (i.e. homeostasis) while neuromodulation may work the cooperation of different positive and negative feedbacks. Furthermore, neural and motor systems may consider robustness over optimality. Nonlinear control theory in limit cycle and alternative rhythmic dynamics need to develop according to linear systems and other shapes of dynamics [78].

In recent time some theoretical control about single neurons [79] [80] [81] [82] and neural clusters [83] [84] [85] have been increased. Additional theoretical studies including optimal control theory to make control inputs that stimulated target spike designs with small energy stimuli applying electrical current in single neurons [80] and neuron populations [81]. Mostly basic models of spiking neural networks [86] are used to similar way powerful computational systems for optimal control and multilinear feedback [87] is used by paired oscillator for individually controlling. Roughly gathering proof propose that in neurons synchronized oscillatory abnormalities can play a role in some brain disease [88] like epilepsy. Beside control of spiking neurons closed-loop optogenetic control [89] [90] for direct goal as oscillations may give considerable results [91].

In recent work [92], the problem of coupled Hodgkin-Huxley phase neurons are described with a single limited input. To find a minimum energy desynchronizing is important for the control. Another various works considered potential desynchronizing for the pathologically synchronized neurons in a population [93] [94]. A number of event-based optimal control theory is considered for single neuron level by [80] [95] [96] [97] [98] [99]. Also [100] have considered inter-spike-interval control problem for minimum and maximum possible time as a limited input on phase models of neurons [101].

The majority of the feed-forward control algorithms have been applied to related spike trains (ST) have constant amplitudes related neuron models with variation over the between spike time and number of spike in series. For example, amplitude-constrained, an ideal control scheme have control current consisting of triangle spike [81] and an alternative to this that one-dimensional, simplified, reduced model analysis [100], a reverse control with added delay on spike trains [86] and finally said that spike train model that predicts the spikes in the living body [102].

The feedback (closed-loop) approach is used experimentally to stimulate non-monotonic firing response in certain situations. A completely different approach was applied in [103], which is a nonlinear control signal designed with the fuzzy interpolation method for HH neurons. The steps are as follows:

- Interpolation of linear stochastic systems,
- To approach nonlinear stochastic HH dynamics using interpolation,
- The method of restoring the control signal from the linear matrix inequality [103], (the MATLAB power control toolbox was used).

The most powerful aspect of such an approach is that it offers the opportunity to overcome the challenges comes from reference-tracking control designed with time-delaying and external noise [104]. The other side, missing aspect of approach is relatively complicated and it is a very time consuming process in numerical analysis.

Thus, as expected, the feedback algorithm set proved to be a more efficient tool for designing arbitrary target outputs. On the other hand, most of the described closed-loop algorithms often deal with two-dimensional differential models of biological neurons and have common handicaps those set points and have limited "attractor" sets such as limit loops [105]. Chaotic situations are not included in this planar set.

The vast majority of publications have concentrated on synchronization with control of spike train and bursts from single neurons. The methods used to achieve such

synchronization include both an open-loop controlled by an external time-periodic signal [106] and closed-loop control. Feedback is usually presented in two simple ways:

- phase and frequency locking [107] [108];
- linear [93] [109] [110] [111] [112] or nonlinear, non-adaptive time-delayed feedback [113] [114].

In particular, it is necessary to mention the synchronous algorithm set from the non-linear stability error signal, which acts as an observer [115]. Time delay correction is the most efficient [116]. The delayed speed gradient method was applied in synchrony with FitzHugh-Nagumo neuron pairs [117]. Although the method works very efficiently, the proposed approach to control the properties of the inter-neuron connections is far from realistic (in reality the connections between neurons are not symmetrical).

Other time-delayed planar models are also found in the literature: Wilson-Cowan neuron network [118], the effect of the stochastic resonance of time delay on planar neuron networks [119]. The control methods mentioned above have been applied to:

- The Plank models [93] [106] [107] [109] [112] [113] [120] [121];
- The three dimensional Hindmarsh-Rose neurons [111] [114] [122] [123];
- The medium spiny neuron model [124].

Simple time-delay synchronization has also been studied for alternative three-dimensional Leech-Heart inter-neurons [125]. Arnold phase lock is given in the superposition of the control current inputs for the *j*-th HH neuron connected to *N* neighbors in the synchronization of HH neuron pairs [126]:

$$I_j = \omega \sum_{k=1}^{N} a_{jk} r_k(t) \cdot (v_j - v_k), \tag{3.1}$$

Match force ω, neighboring matrix element a_{jk}, *k-th* neuron action potential is v_k, *j-th* neuron ligand receptor fraction $r_k(t)$; because of $r(t)$ is a tuned non-linear function, the control is not adaptive [126] and the required diversity of dynamic states cannot be produced efficiently.

The linear structures of the block-diagram feedback for the synchronization of the HH neuron are filtered by two-stage state control [127] and second linear estimator (Kaman filter), filters [128] or erosion filters [129] [130].

Although the effectiveness of the methods have been outlined above we must point out here that the goal of this thesis is not just to synchronize pulses designed in the frame of HH neuron's own dynamics. We want to force the arbitrary constructed goal dynamical regime on the Hodgkin-Huxley system to provide the aimed spiking or bursting of a single HH neuron and, then, a collective spiking of their clusters by manipulating with dynamical features of one (or few) given neuron from the cluster. Among the proposed algorithms SG and TA seem to be the most convenient for this goal, they also simply facilitate the further development like covered noisy components and time delay.

3.2 Speed Gradient algorithm

The speed-gradient (SG) algorithm is a competent method to solve a variety of nonlinear and adaptive estimation and control problems for physical and mechanical systems [131] [132] [133] [134]. The speed gradient (SG) algorithm is based on the definition of the scalar target function [135] [136] that a single neuron with an action potential can be defined as:

$$G = \frac{1}{2}\left[v(t) - v_*(t)\right]^2. \tag{3.2}$$

Here, $v(t)$ is the actual action potential in the system while $v_*(t)$ is a target potential should have a shape of a properly differentiable function.

The purpose of feedback control is achieved when the target function G go to the zero. As a given time-dependent function, the specific target that track the target membrane potential v^* is called tracking. Let's take the time derivative of Eq. (3.2):

$$\Omega = \frac{dG}{dt} = (v(t) - v_*)\left[\frac{dv}{dt} - \frac{dv_*}{dt}\right]. \tag{3.3}$$

The derivative dv/dt , includes the control signal I along the right side of the Eq. (2.4) corresponding to the dynamic system. The algorithm defines the feedback control in the form of a gradient in the control signal field. In the case of a single neuron, the

driving current I is converted to a partial derivative due to the 1-dimensional character of I:

$$I_{\mathrm{SG}} = -\gamma \frac{\partial \Omega}{\partial I} \tag{3.4}$$

Here γ is a positive constant, denoted by Eq. (2.4):

$$I_{\mathrm{SG}} = -\frac{\gamma}{C_M}(v - v_*) \ . \tag{3.5}$$

Along with the system Eq. (2.4), the SG control algorithm Eq. (3.5) directs the evolution of the dynamic system to the attractor manifold defined by the target function Eq. (3.2).

3.3 Target Attractor algorithm

The target attractor algorithm ("synergetic control" in the author's terminology) is based on "directed self-organization of the dynamic system". Synergetic control (SC) applied to equations of nonlinear, multidimensional, multiply linked dynamical systems for solving. Synergetic control theory have used successfully in many nonlinear technical objects like that flying apparatus, turbo generators, robots, electric drives, technological aggregates etc. and in the ecology, biotechnology etc. for control of the complex problems [137]. SC optimizes the behavior of systems such as bifurcations and phase transitions, unwanted and dangerous attractors in their state space, non-uniqueness of the solution of control task, etc. SC provides to construct objective control rules, for the advanced mathematical models without using the linearization processes or other simplifications. m-parametric attracting invariant manifold (subset specifying control target):

$$\psi_s(x_1,...,x_n) = 0 \ ; \ s = 1...m \tag{3.6}$$

$x_1,\ldots,x_n$ are defined as a function of the state variables. Eq. (3.6) provide asymptotic stability of the system dynamics according to the control objective. To do this, we would like to perform the following optimizer functions:

$$J = \int_0^{\infty} \left(\sum_{s=1}^{m} \left[T_s^2 \left(\frac{d\psi_s(t)}{dt} \right)^2 + \psi_s^2(t) \right] \right) dt = \min \ . \tag{3.7}$$

Here T_s, is a positive constant (time scales). To obtain a minimum Eq. (3.7) in exponential asymptotics, we define "synergetic" feedback as a series of equations for s for the observers[138]:

$$T \frac{d\psi_s(t)}{dt} + \psi_s(t) = 0 \tag{3.8}$$

Observers tend to zero Eq. (3.6), directs the dynamic development of the system to the attractive targets Eq. (3.8).

We applied a target attractive feedback algorithm for the membrane potential *v(t)*. We define the target function for its following:

$$\psi(t) = v(t) - v_*(t) \tag{3.9}$$

with a given target potential *v*(t)*. The "synergetic" feedback in the exponential form Eq. (3.8) is given by:

$$T \frac{d\psi}{dt} = -\psi \tag{3.10}$$

with a positive control constant *T*. This cause to:

$$\frac{dv}{dt} = \frac{dv_*}{dt} - \frac{1}{T}(v - v_*) \ . \tag{3.11}$$

After the control signal *I* has been put in place Eq. (3.11), it is brought from the right side of the dynamic system to its previous state Eq. (2.4):

$$I_{\mathrm{TA}} = C_M \cdot \left[\frac{dv_*}{dt} - \frac{1}{T}(v - v_*) \right] + g_{Na} m^3 h \cdot (v - E_{Na}) + g_K n^4 \cdot (v - E_K) + g_{Cl} \cdot (v - E_{Cl}) . \tag{3.12}$$

Equation (3.12), along with system Eq. (2.4), refers to the target action potential *v** in the followed by the driven neuron.

3.4 Numerical simulations

The tracking difference for the two algorithms is presented for the target signal *v** in Figure 3.1:

$$v_*(t) = \cos t - 3\cos(\sqrt{5}t - 2) + 3\cos(-7t - 0.5) + \cos(\pi \cdot t + 1) - 0.3\cos\left(\frac{13}{21}t + 5\right) + Vrest\ . \quad \textbf{(3.13)}$$

The typical scale of the target function Eq. (3.13) reflects the properties of real neurons. The control constants for SG and TA algorithms were chosen respectively as gamma γ=30 and 1/*T*=1/30.

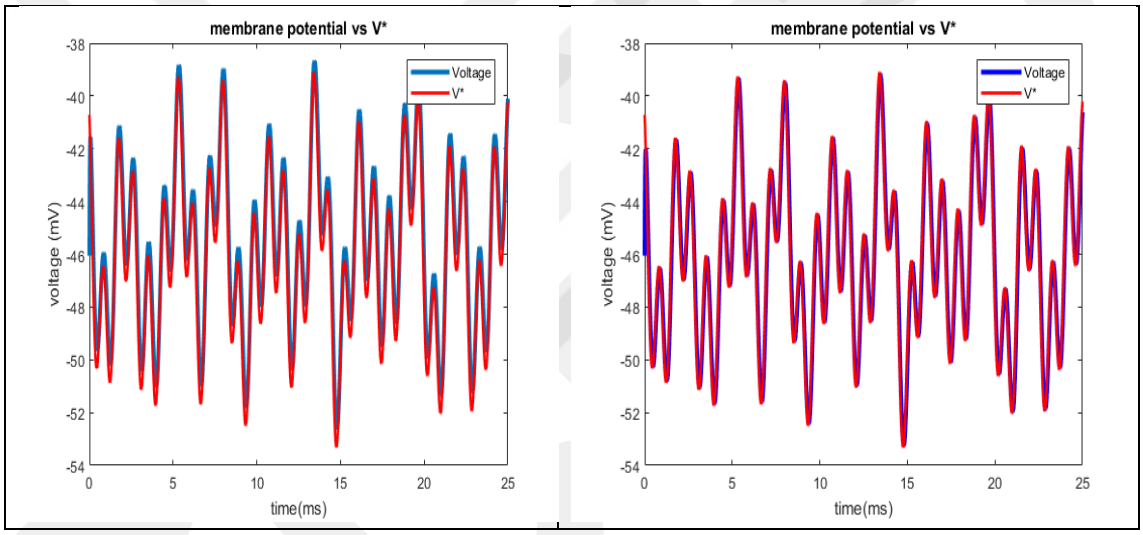

Figure 3.1: Tracking for the linear superposition of harmonics Eq. (3.13).The target potential *v*(t)* is denoted by red color, the actual action potential *v(t)* – by blue color. **Left:** speed gradient algorithm; **Right:** target attractor algorithm.

At the points with the highest absolute value of the target potential derivative TA algorithm follows the target potential better than SG method.

Here is the control parameter as current *I(t)*;

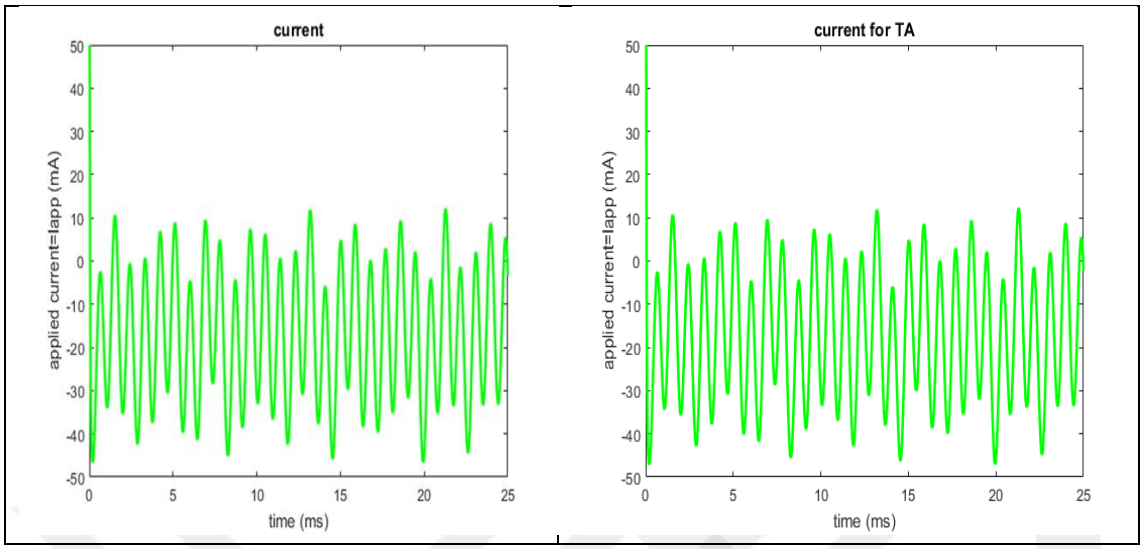

Figure 3.2: Control parameter current as *I(t)* for the tracking goal Eq. (3.13). **Left:** speed gradient algorithm; **Right:** target attractor algorithm.

On Figure 3.3 the tracking is performed for the combination of a burst-type function and the train of three Gaussian-shaped spikes:

$$v_*(t) = (\sin(8\pi t) + 6) \cdot \exp\left\{-\frac{(t-2)^2}{5}\right\} + \exp\left\{-\frac{(t-8)^2}{5}\right\} + \\ + \exp\left\{-\frac{(t-10)^2}{5}\right\} + \exp\left\{-\frac{(t-18)^2}{5}\right\} + Vrest. \qquad \textbf{(3.14)}$$

They correspond to a combination of bursting and spiking behavior in the real neuron. The control constants for SG and TA algorithms were chosen respectively as gamma γ=30 and $1/T$=1/30.

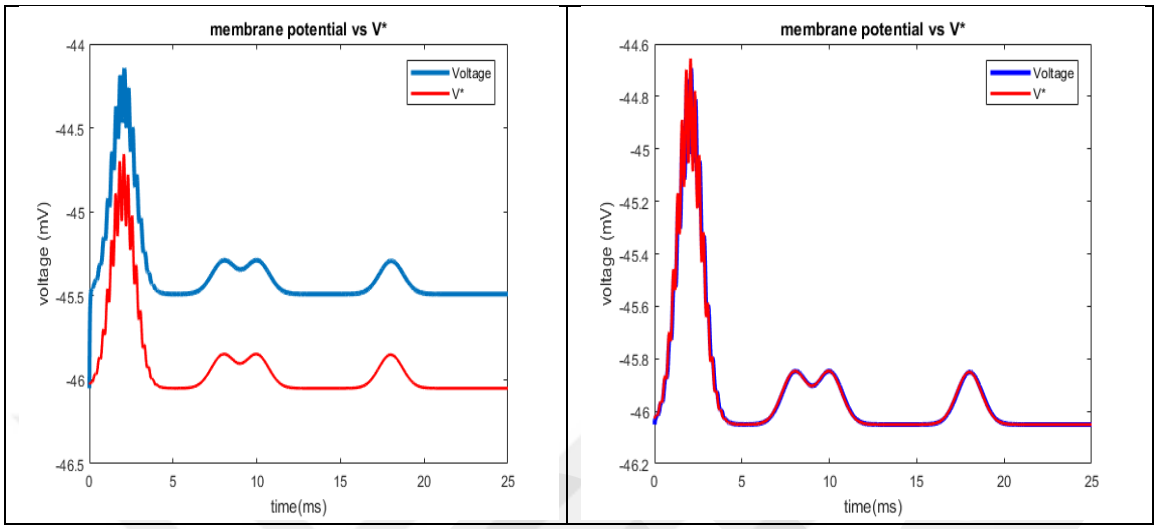

Figure 3.3: Tracking for the burst-type pulse and the spike train Eq. (3.14).The target potential *v*(t)* is denoted by red color, the actual action potential *v(t)* – by blue color. **Left:** speed gradient algorithm; **Right:** target attractor algorithm.

It is easy to see that the speed gradient algorithm can model the random shape of the target potential, but there may be a systematic error between the actual action potential (blue color in Figures 3.1 and 3.3) and the target (red color in Figures 3.1 and 3.3). The target attractor algorithm does not indicate these features. Almost it tracked one to one desired potential in Figures (3.1 and 3.3).

3.5 Tracking error of control

The goal achievement of the tracking is evaluated by the error function:

$$e(t) = \left| v(t) - v_*(t) \right| . \tag{3.15}$$

The errors are plotted for the target functions Eq. (3.13) and Eq. (3.14) on Figure 3.4.

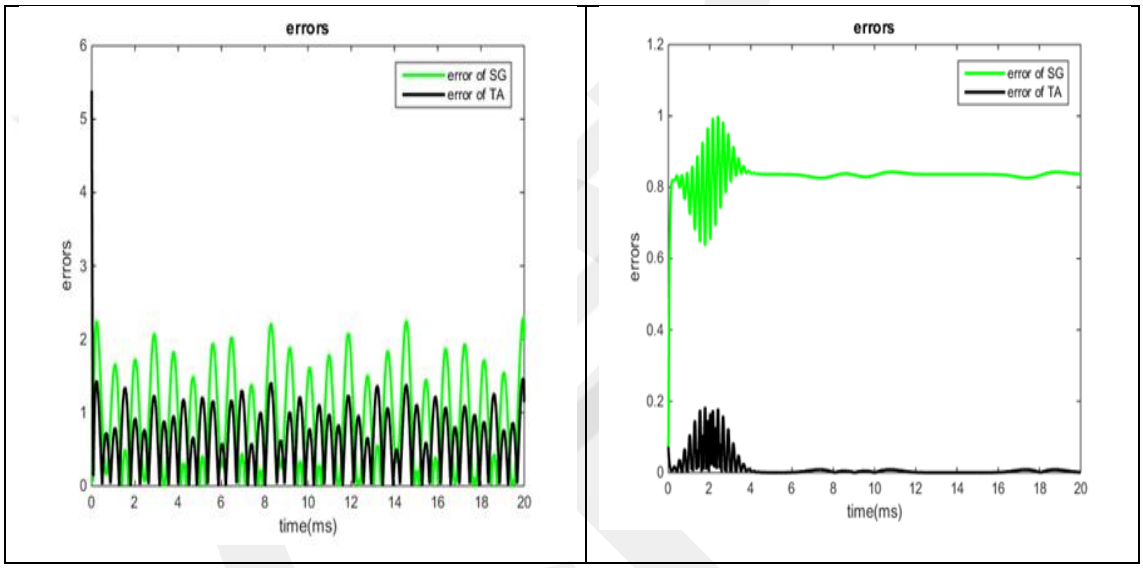

Figure 3.4: Error of tracking *e(t)* for speed gradient (green) and target attractor (black) algorithms. **Left:** the linear superposition of harmonics Eq. (3.13); **Right:** the bursting-and-spiking train Eq. (3.14) [139].

On Figure 3.4 one can easily defined that the success of the goal may have the systematic error for the state of SG, especially for the spiking train example. It changes strongly according to the control constant gamma in Figure 3.3. This effect is observed for the speed gradient algorithm only, see Figure 3.5 below. On the other hand the target attractor algorithm leads to the minor error because of the tracking goal exponentially fast.

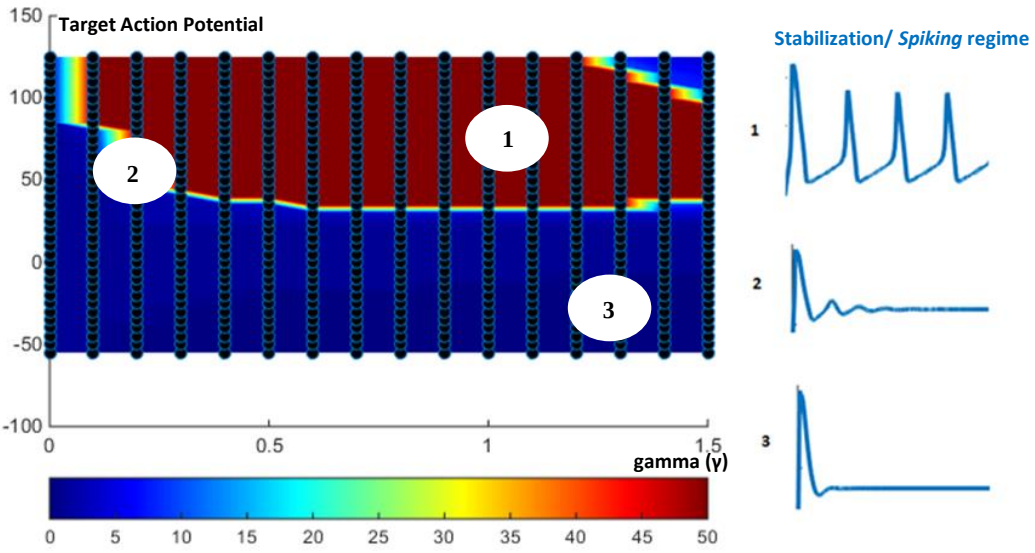

Figure 3.5: The achievability of the control goal Eq. (3.2) in speed gradient algorithm for different control constants as gammas *(γ)*. **Horizontal axis:** gamma constant in Eq. (3.4); **Vertical axis:** the stabilization level *v**. The color marks the quality of the stabilization (see the explanations above) [139].

We investigated the presence of the systematic error for SG algorithm taking the target signal *v** as a constant, i.e. considering the case where the tracking goal is just a stabilization of the action potential at the certain level. The horizontal axis on Figure 3.5 represents different gammas (normalized by the capacitance *Cm*), while the vertical axis stands for the target level of the action potentials at which we desire to stabilize the system. The color marks the approximate number of oscillations for the dynamics of the actual action potential *v(t)* around the stabilization level *v**. The deep blue asymptotic color is numbered 3 spiking regime reflects to a perfect stabilization, while the deep red asymptotic color is numbered 1 spiking regime represents non-decaying oscillations of the action potential around the target level that never leads to the stabilization. Rest, between number 1 and number 3, transition region is numbered 2 spiking regime shows a number of spiking after that it reaches to stabilization with decreasing spiking regime.

Thereby, on Figure 3.5 shows that the choice of the control parameter as the gamma γ must be in a good harmony with the target level of the action potential *v**, or else there is no the target achievement (the red domain on the plot). The similar impact defined on the right plot of Figure 3.4 for SG case.

3.6 Energy power of control

Another important principle of successful control is the minimum power of the energy *P(t)* that is pumped by the control field into the system per unit of time. For the HH electrical circuit model providing the dynamical system Eq. (2.4) it can be calculated as:

$$P(t) = I(t)v(t). \tag{3.16}$$

For the particular target potential cases Eq. (3.13) and Eq. (3.14), these powers are plotted on Figure 3.6.

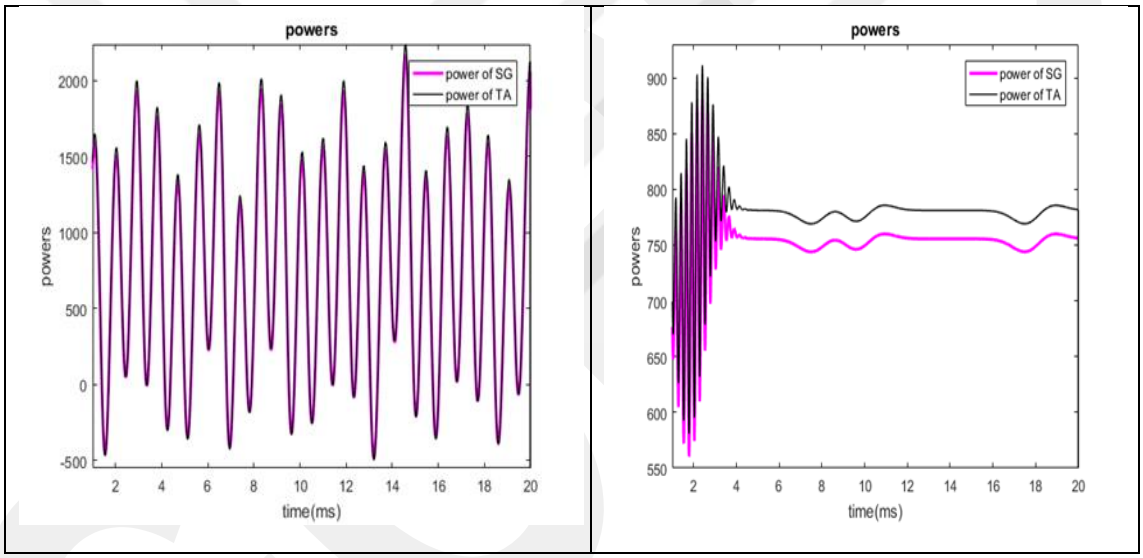

Figure 3.6: Power of tracking *P(t)* for speed gradient (pink) and target attractor (black) algorithms. **Left:** the linear superposition of harmonics Eq. (3.13); **Right:** the bursting-and-spiking train Eq. (3.14) [139].

The power of SG doesn't differ from the power of TA signals adequately for the harmonic target (the left plots). Nevertheless, for another target potential as spiking and bursting trains (the right plots) the target attractor algorithm seems to be more energy consuming: the corresponding black curve of the energy pumping by control systematically stays above the SG pink curve.

3.7 Comparison of two methods and conclusions

To point out the fundamental difference between two control algorithms, SG and TA, we express those terms in mechanic.

Speed gradient algorithm generates an extra force that serves as a ‘viscous friction’ in the dynamical system. It is off at the constant or dynamically altering goal parameter level (action potential in our model). Far away from this level the ‘friction’ is growing.

Target attractor algorithm describes the attractor manifold, gets the dynamics of the system into its neighborhood exponentially and urges the system to keep always at the target attractor. Absolutely, such a’ hard’ approach should be more efficient from the view of accuracy to compare with the ‘soft’ SG, but in the same time more energy consuming.

Both algorithms give the robustness [135] they do not depend adequately on the initial conditions and are stable under the relatively small external perturbations in the dynamics of the driven system Eq. (2.4). Both algorithms are sub-optimal: they are closed to the Pontryagin’s optimal control locally.

We do not know exactly the set of the initial conditions for the dynamical variables Eq. (2.4) for real neurons. Actually initial conditions change for each real neuron according to type of the living. In the frame of SG and TA algorithms it is not enough, because the behavior of the dynamical system depends on the initial conditions of system [24]. As an example, we demonstrate on Figure 3.7 the dynamics of the system Eq. (2.4) with few sets of its initial conditions under SG tracking (the target potential is colored by red).

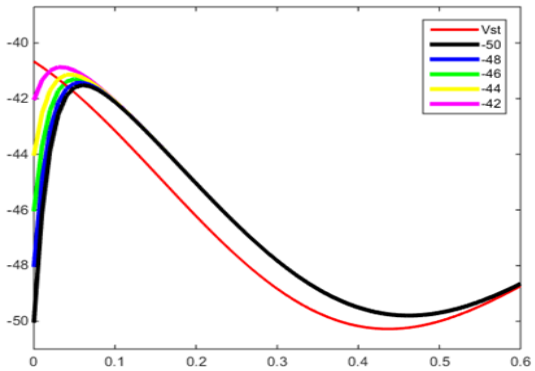

Figure 3.7: SG tracking of the target signal (red line) for different initial conditions; **Vertical axes:** the potantials in mV; **Horizontal axes:** time in ms [139].

The Figure 3.7 demonstrates that all initial conditions in the system dynamics converged to the target behavior.

The simulation results exhibit the effectiveness of such theoretic analysis and control methods. This new combine study that HH neuron model and control algorithms as SG and TA give great result. If we want to minimum error for track to target potential we should choose TA but if desire to less energy and time consuming control we could choose SG.

Chapter 4

Tracking in HH Neuron Populations

4.1 Tracking in linear chains

To build up a neural chain we need two main elements:

1. HH mathematical neuron controlled by the external input *I* via SG or TA algorithm;
2. The 'synaptic' transfer element that defines the input I_k of the next *k*-th from the output action potential $V_{(k-1)}$ of the previous *(k –1)*-th neuron in the chain.

For the HH element we use the same model as Eqs. (2.4a-2.4b):

$$\begin{aligned}
&C_M \cdot \frac{dv_k}{dt} = -g_{Na} m_k^3 h_k \cdot (v_k - E_{Na}) - g_K n_k^4 \cdot (v_k - E_K) - g_{Cl} \cdot (v_k - E_{Cl}) + I_k \ ; \\
&\frac{dm_k}{dt} = \alpha_m(v_k) \cdot (1 - m_k) - \beta_m(v_k) \cdot m_k \ ; \\
&\frac{dn_k}{dt} = \alpha_n(v_k) \cdot (1 - n_k) - \beta_n(v_k) \cdot n_k \ ; \\
&\frac{dh_k}{dt} = \alpha_h(v_k) \cdot (1 - h_k) - \beta_h(v_k) \cdot h_k \ .
\end{aligned} \qquad \textbf{(4.1)}$$

Here $V_k(t)$ stands for the action potential of the *k*-th neuron, $m_k(t)$, $n_k(t)$, $h_k(t)$ are its gate variables, and the control signal is represented by the sum of *I(t)* external currents entering the *k*-th cell.

The second element, transferring the electrical stimulation from the axon of *(k –1)*-th neuron to the input of *k*-th neuron via synapses, dendrites and soma of the *k*-th cell, maybe chosen in different manner, including a time delay reaction or existing of a threshold accumulating the inputs coming from the dendrites to soma. Here we use the gain model:

$$I_k(t) = \alpha \cdot [v_{k-1}(t) - v_{\text{rest}}]; \ \alpha = \text{const} > 0. \qquad \textbf{(4.2)}$$

The model Eq. (4.2) has a modification with time delay τ:

$$I_k(t) = \alpha \cdot [v_{k-1}(t-\tau) - v_{\text{rest}}]\ ;\ \alpha = \text{const} > 0, \tag{4.3}$$

It includes internal processes related to signal coming from dendrites to soma.

Apart from Eq. (4.2), the first control current I_1 must be restored as the general control signal $I(t)$, while the general output is given by $V_N = v^*(t)$, where $k = 1, 2, \ldots, N$; and N is the number of HH neurons in the chain. Thus, the first element of the chain must track the dynamical behavior for its last element. Algorithmically, the control in the chain has a back spread: first we restore the target I_N for tracking V_N, i.e. v^*, by Eq. (4.2) it defines the new target $V_{(k-1)}$, again in the frame of SG and TA algorithms we restore the target control $I_{(k-1)}$, and so on up to the first cell, for which we finally get the external control $I(t)$.

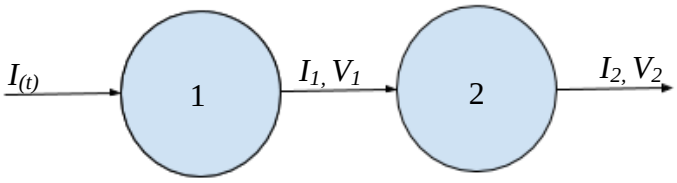

Figure 4.1: Basic model of pair of HH neurons

For the pair of HH neurons we can show the elements Eq. (4.1) and Eq. (4.2) in the form:

$$
\begin{aligned}
&C_M \cdot \frac{dv_1}{dt} = -g_{Na} m_1^3 h_1 \cdot (v_1 - E_{Na}) - g_K n_1^4 \cdot (v_1 - E_K) - g_{Cl} \cdot (v_1 - E_{Cl}) + I(t)\ ;\\
&\frac{dm_1}{dt} = \alpha_m(v_1) \cdot (1 - m_1) - \beta_m(v_1) \cdot m_1\ ;\\
&\frac{dn_1}{dt} = \alpha_n(v_1) \cdot (1 - n_1) - \beta_n(v_1) \cdot n_1\ ;\\
&\frac{dh_1}{dt} = \alpha_h(v_1) \cdot (1 - h_1) - \beta_h(v_1) \cdot h_1\ ;\\
&v_{1,*} = \frac{1}{\alpha} I_2; \qquad \textbf{(4.4)}\\
&C_M \cdot \frac{dv_2}{dt} = -g_{Na} m_2^3 h_2 \cdot (v_2 - E_{Na}) - g_K n_2^4 \cdot (v_2 - E_K) - g_{Cl} \cdot (v_2 - E_{Cl}) + I_2\ ;\\
&\frac{dm_2}{dt} = \alpha_m(v_2) \cdot (1 - m_2) - \beta_m(v_2) \cdot m_2;\\
&\frac{dn_2}{dt} = \alpha_n(v_2) \cdot (1 - n_2) - \beta_n(v_2) \cdot n_2\ ;\\
&\frac{dh_2}{dt} = \alpha_h(v_2) \cdot (1 - h_2) - \beta_h(v_2) \cdot h_2\ ,
\end{aligned}
$$

Alpha α is the transition coefficient that provides transition of electrical potential from *(k-1)*-th neuron to *k*-th neuron.

Where the currents are given by Eq. (3.5) for speed gradient method:

$$
\begin{aligned}
&I(t) = -\frac{\gamma}{C_M}(v_1 - v_{1,*}); \qquad \textbf{(4.5)}\\
&I_2 = -\frac{\gamma}{C_M}(v_2 - v_*),
\end{aligned}
$$

or by Eq. (3.12) for target attractor method:

$$I(t) = C_M \cdot \left[\frac{dv_{1,*}}{dt} - \frac{1}{T}\left(v_1 - v_{1,*}\right) \right] + g_{Na} m_1^3 h_1 \cdot (v_1 - E_{Na}) +$$
$$+ g_K n_1^4 \cdot (v_1 - E_K) + g_{Cl} \cdot (v_1 - E_{Cl}) ;$$

$$I_2 = C_M \cdot \left[\frac{dv_*}{dt} - \frac{1}{T}\left(v_2 - v_*\right) \right] + g_{Na} m_2^3 h_2 \cdot (v_2 - E_{Na}) + \quad \textbf{(4.6)}$$
$$+ g_K n_2^4 \cdot (v_2 - E_K) + g_{Cl} \cdot (v_2 - E_{Cl}) .$$

The tracking behaviors in the linear chain for both algorithms are presented for the target signal *v** in Figure 3.1.

The typical scale of the target function Eq. (3.13) (see Chapter 3) reflects the properties of real neurons. The control constants for two algorithms SG and TA were chosen respectively as, gamma γ=30 and 1/*T*=1/30. Additionally, transition coefficient alpha was chosen α=1.

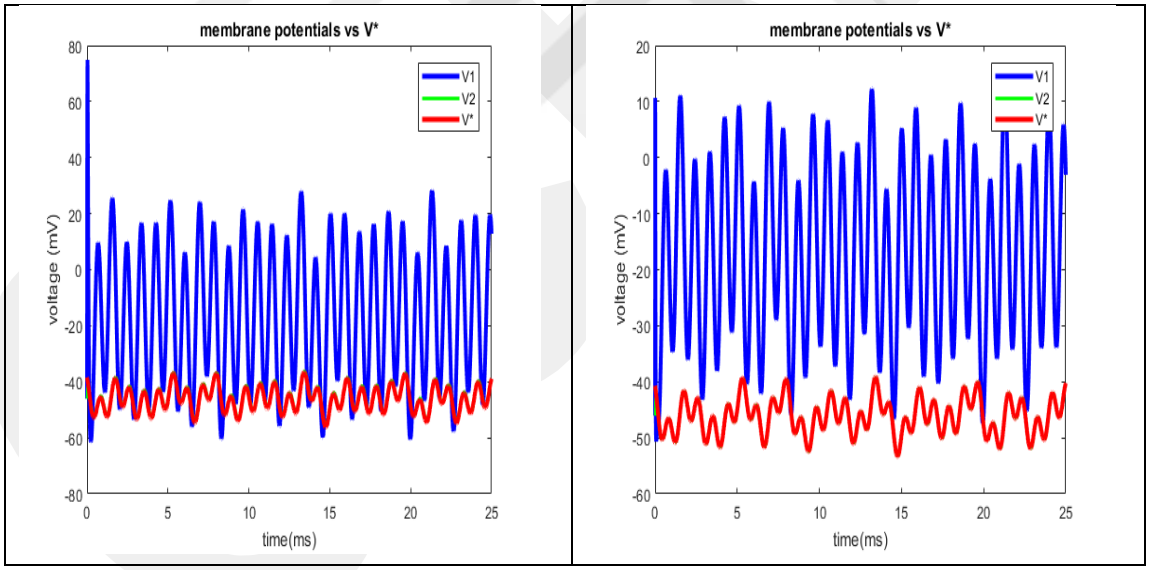

Figure 4.2: Tracking for the linear superposition of harmonics Eq. (3.13).The target potential *v*(t)* is denoted by red color, the actual action potential for first neuron *v1*– by blue color. The actual action potential for second neuron *v2*– by green color **Left:** speed gradient algorithm; **Right:** target attractor algorithm.

In these drawing, the action potential V_2 follow the target potential *v* * with an error not exceeding 4%. Thus, simulations are showing that TA algorithm follow the goal potential better than SG used in the linear chain

Here is the control parameter as current *I(t)* for both algorithm in the linear chain;

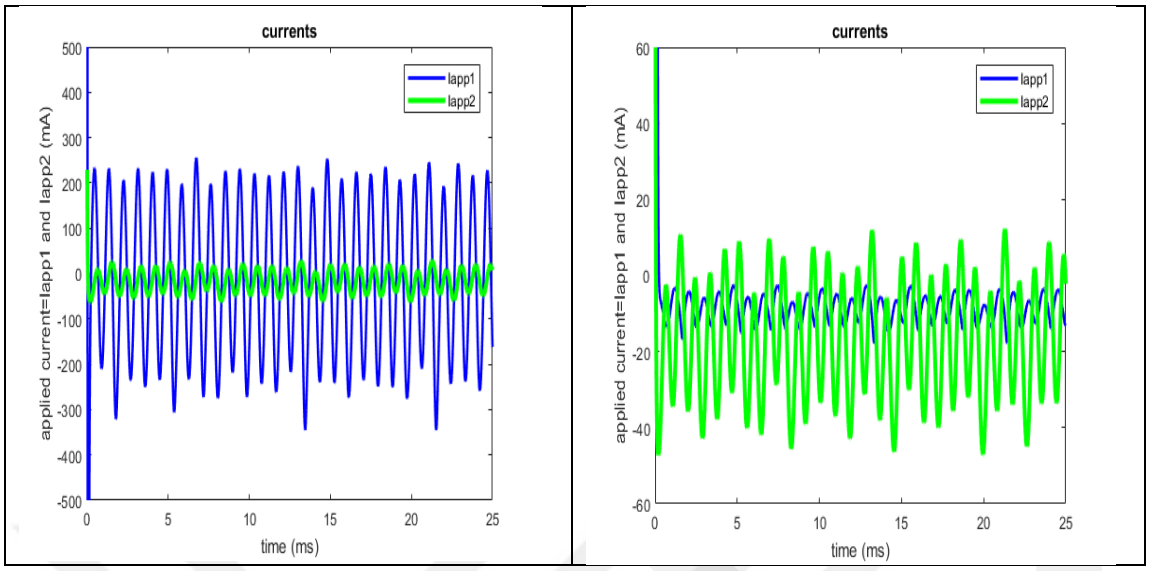

Figure 4.3: Control parameter current as *I(t)* for the tracking goal in linear chain Eq. (3.13). **Left:** speed gradient algorithm; **Right:** target attractor algorithm.

But the existence of the supporting goal function *v1** in the TA algorithm Eq. (4.6) enlarges drastically the simulation duration for the pair of neurons. This problem will increase with the extension of the number of neurons in the linear chain and, later, in the ring configurations.

Also we have experimented linear chain with three and four neuron for both algorithms we obtain similar results tracking the pair of neuron.

4.2 Tracking in linear chains with loops

Here we construct the elements in form for the simplified configuration of the HH neuron pair coupled into the closed loop that is feedback.

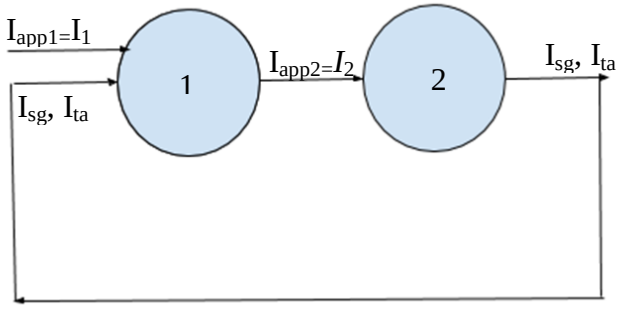

Figure 4.4: Basic model of pair of HH neurons with loop

$$C_M \cdot \frac{dv_1}{dt} = -g_{Na} m_1^3 h_1 \cdot (v_1 - E_{Na}) - g_K n_1^4 \cdot (v_1 - E_K) - g_{Cl} \cdot (v_1 - E_{Cl}) + I(t) + I_1;$$

$$\frac{dm_1}{dt} = \alpha_m(v_1) \cdot (1 - m_1) - \beta_m(v_1) \cdot m_1 ;$$

$$\frac{dn_1}{dt} = \alpha_n(v_1) \cdot (1 - n_1) - \beta_n(v_1) \cdot n_1 ;$$

$$\frac{dh_1}{dt} = \alpha_h(v_1) \cdot (1 - h_1) - \beta_h(v_1) \cdot h_1 ;$$

$$v_{1,*} = \frac{1}{\alpha} I_2; \qquad \textbf{(4.7)}$$

$$C_M \cdot \frac{dv_2}{dt} = -g_{Na} m_2^3 h_2 \cdot (v_2 - E_{Na}) - g_K n_2^4 \cdot (v_2 - E_K) - g_{Cl} \cdot (v_2 - E_{Cl}) + I_2 ;$$

$$\frac{dm_2}{dt} = \alpha_m(v_2) \cdot (1 - m_2) - \beta_m(v_2) \cdot m_2 ;$$

$$\frac{dn_2}{dt} = \alpha_n(v_2) \cdot (1 - n_2) - \beta_n(v_2) \cdot n_2 ;$$

$$\frac{dh_2}{dt} = \alpha_h(v_2) \cdot (1 - h_2) - \beta_h(v_2) \cdot h_2;$$

$$I_1 = \alpha \cdot v_* .$$

where the currents are given by Eq. (3.5) for speed gradient method:

$$I(t) = Isg + I_1;$$

$$I_2 = -\frac{\gamma}{C_M}(v_2 - v_*), \qquad \textbf{(4.8)}$$

$$Isg = -\frac{\gamma}{C_M}(v_1 - v_{1,*})$$

or by Eq. (3.12) for target attractor method:

$$I(t) = Ita + I_1;$$

$$I_2 = C_M \cdot \left[\frac{dv_*}{dt} - \frac{1}{T}(v_2 - v_*) \right] + g_{Na} m_2^3 h_2 \cdot (v_2 - E_{Na}) +$$
$$+ g_K n_2^4 \cdot (v_2 - E_K) + g_{Cl} \cdot (v_2 - E_{Cl}) \ . \qquad \textbf{(4.9)}$$

$$Ita = C_M \cdot \left[\frac{dv_*}{dt} - \frac{1}{T}(v_1 - v_{1,*}) \right] + g_{Na} m_1^3 h_1 \cdot (v_1 - E_{Na}) +$$
$$+ g_K n_1^4 \cdot (v_1 - E_K) + g_{Cl} \cdot (v_1 - E_{Cl}) \ ;$$

The numerical results of the tracking for the pair of loop-coupled HH neurons are represented on Figures 4.5-4.6 for speed gradient algorithm and target attractor algorithm. As a target voltage function we use here the signal Eq. (3.13).

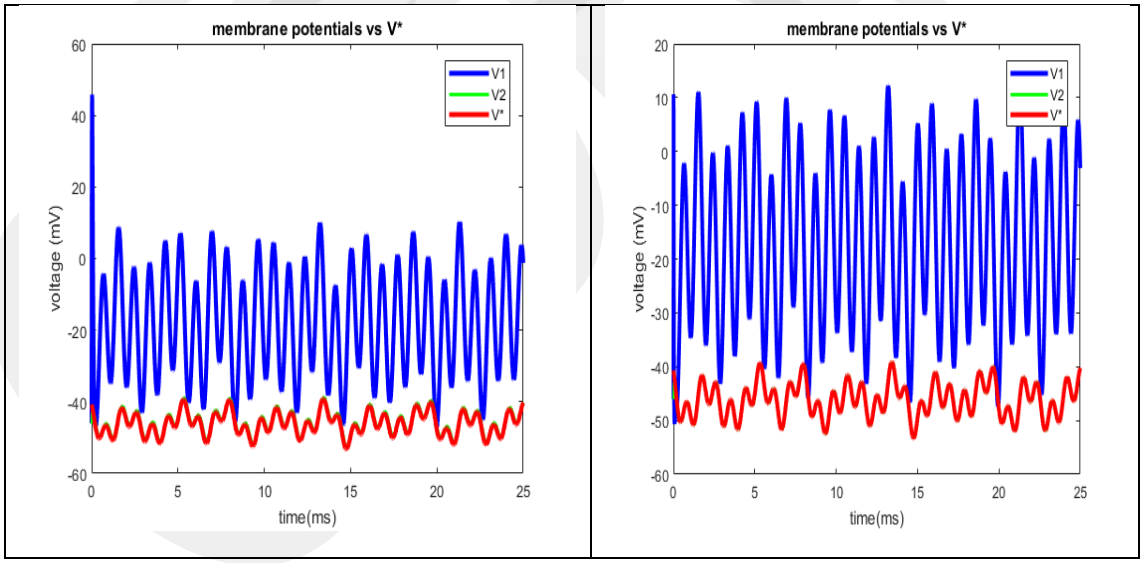

Figure 4.5: Tracking for the linear superposition of harmonics Eq. (3.13).The target potential *v*(t)* is denoted by red color, the actual action potential for first neuron *v1*– by blue color. The actual action potential for second neuron *v2*– by green color **Left:** speed gradient algorithm; **Right:** target attractor algorithm.

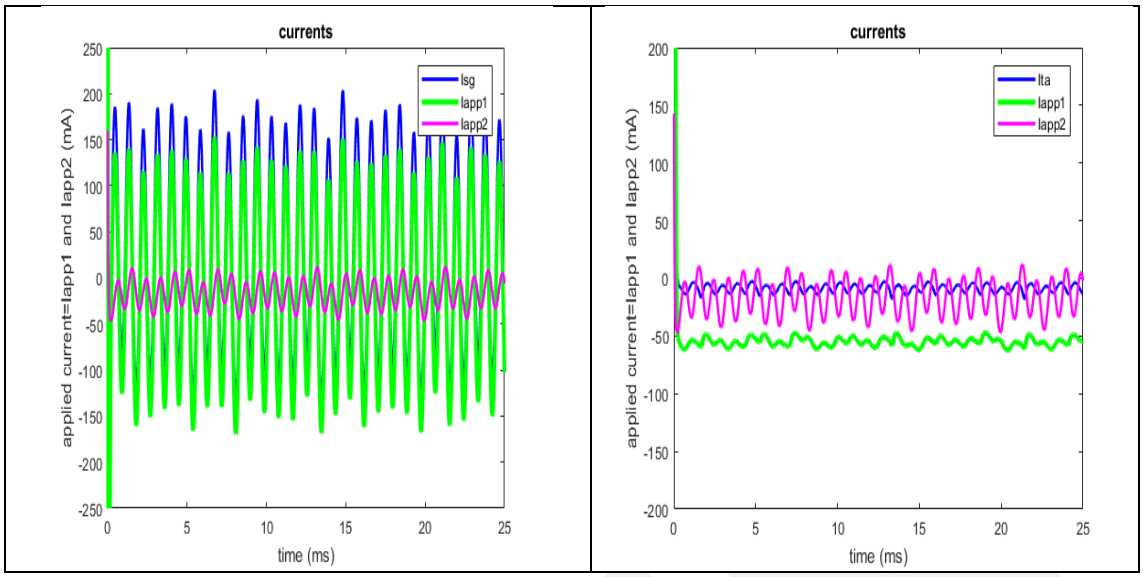

Figure 4.6: Control parameter current as I(t) for the tracking goal in close loop Eq. (3.13). **Left:** speed gradient algorithm; **Right:** target attractor algorithm.

For the loop of two neurons we did not observe any additional features in the applications of SG or TA algorithms. Simulations show that TA algorithm better tracking of target potential and SG algorithm faster than TA algorithm.

We checked loops of three and four neurons for both algorithms we did similar results loop of two neurons.

One of the main issues in the loop architecture is: nonlinear links between HH neurons in 3- and 4-neuron cycles can produce the effect of stable common fluctuations similar to those observed in the famous numerical Fermi-Paste-Ulam experiment. The open question is whether there is a fundamental difference between the monitoring of HH neuronal cycles in open linear HH chains. Numerical stimuli show that there is no such effect for our using control algorithms.

4.3 Suppressing epileptiform behavior in HH neurons via SG algorithms

Epilepsy is a seizure disorder in the brain. It usually starts unannounced, disrupting normal brain functions and can be fatal, threatening the patient's life, personal life, memory, and mental functions. Actual mechanism underlying the epilepsy is not known exactly. But it can has a number of reasons such that genetic factor, head

injury, stroke, birth trauma, infection, brain tumor, some drugs, alcohol, stress and lack of sleep etc. [140].

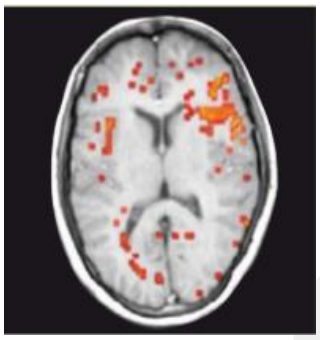

Figure 4.7: This color-enhanced brain scan of a person with epilepsy reveals that the focus of seizure activity is in the right frontal lobe, as shown by the large orange cluster at the top right of the image [140].

Commonly, epileptic seizures divide into two main categories: generalized seizures and partial seizures (see Figure 4.8). Initially, seizures often are beginning in a part of the brain, which might include scar tissue or some structural abnormality, and then spread throughout the rest of the brain.

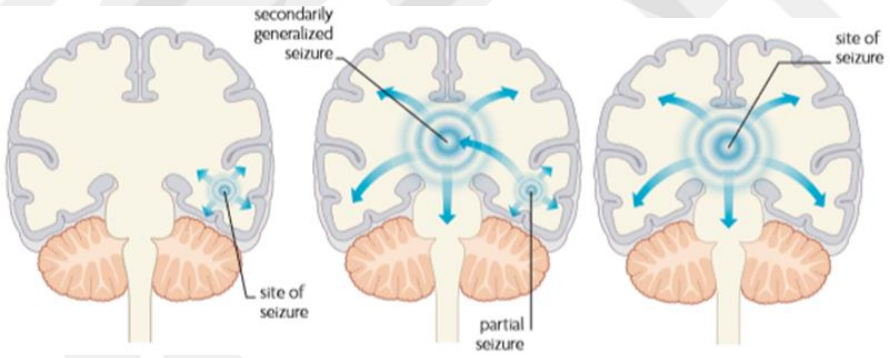

Figure 4.8: Partial and Generalized Seizure [140].

Partial Epileptic Seizures: the seizure starts in and affects only part of the brain (above left). Sometimes, a seizure may begin as a partial seizure and then turn into generalized and spread to whole brain (above right).

Generalized Epileptic Seizures: the seizure affects most or all of the brain with abnormal neuron activity [140].

According to the world health organization (WHO) in the world 65 million while 700 thousand people have epilepsy in Turkey also. Modern neuroscience shows big

development in the study of the collective chaotic states of biological neurons, but the mathematical modeling has not yet succeeded sufficient progress [141]. Many HH neurons chain in epileptiform case shows great concurrence in the invivo animal recordings [142] [143]. The Hodgkin-Huxley dynamic system includes some possible cases of collective bursting ion channel mutations and fluctuations in ion concentration in and out of the axon [144].

Fradkov's speed gradient feedback [24] was applied to check the collective bursting in the Hodgkin-Huxley neuron cluster using the potential action at the moment. The algorithm makes it possible to suppress the traces of chaotic situations, to switch between normal and chaotic situations, and to be suppressed by stimulation of collective bursting.

The proposed algorithm can be used efficiently for studying, identifying and suppressing sudden spiking and bursting epileptic behavior in biological neuronal networks [144].

Here we present a basic model for epileptiform suppression. Consider a sub-cluster of three HH neurons [145], the configuration presented in Figure 4.9.

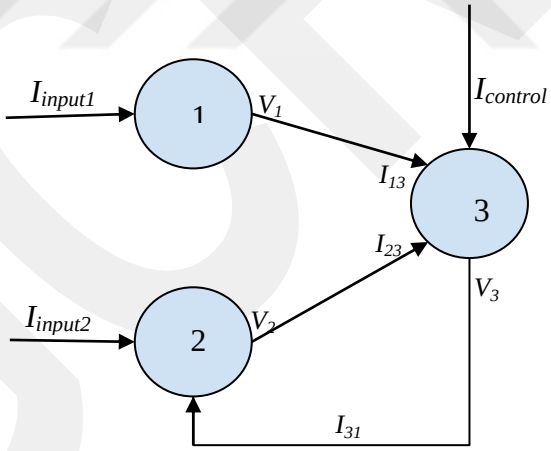

F$_i$gure 4.9: Basic model for an epileptiform suppression in the cluster of three Hodgin-Huxley neurons

In this figure, the neurons 1 and 2 are involved into the collective bursting stimulated by the currents I_{input1} and I_{input2} coming from other companion cells in the neural population. The neuron 3 is a monitoring element providing the switch on and off for the algorithm of suppression. It plays two roles. First, it detects the over-synchronization of the signals coming from the neurons 1 and 2 through the input currents I_{13} and I_{23} (sure, the neurons 1 and 2 may also stimulate other neurons in the

bigger neuron cluster, they are not shown on Figure 4.9). Second, if the neuron 3 observes the over-synchronization in a certain interval of time, it triggers the control algorithm of the suppression through the feedback loop to the neuron 2 by the current I_{31}. The control current $I_{control}$ reflects the inner degree of freedom for the neuron 3. Thus, this element works as an automat driving the neuron 2 from the bursting regime to the resting if and only if it detects its over-synchronization with the neuron 1.

Here we made coupled differential equations that has shown Figure 4.9 basic model;

$$
\begin{aligned}
C_M \cdot \frac{dv_1}{dt} &= -g_{Na} m_1^3 h_1 \cdot (v_1 - E_{Na}) - g_K n_1^4 \cdot (v_1 - E_K) - g_{Cl} \cdot (v_1 - E_{Cl}) + \\
&\quad + I_{\text{input1}} \; ; \\
C_M \cdot \frac{dv_2}{dt} &= -g_{Na} m_2^3 h_2 \cdot (v_2 - E_{Na}) - g_K n_2^4 \cdot (v_2 - E_K) - g_{Cl} \cdot (v_2 - E_{Cl}) + \\
&\quad + I_{\text{input2}} + I_{31} ; \\
C_M \cdot \frac{dv_3}{dt} &= -g_{Na} m_3^3 h_3 \cdot (v_3 - E_{Na}) - g_K n_3^4 \cdot (v_3 - E_K) - g_{Cl} \cdot (v_3 - E_{Cl}) + \\
&\quad + I_{13} + I_{23} + I_{\text{control}} \; ; \\
\frac{dm_k}{dt} &= \alpha_m(v_i) \cdot (1 - m_k) - \beta_m(v_k) \cdot m_k \; ; \\
\frac{dn_k}{dt} &= \alpha_n(v_k) \cdot (1 - n_k) - \beta_n(v_k) \cdot n_k ; \\
\frac{dh_k}{dt} &= \alpha_h(v_k) \cdot (1 - h_k) - \beta_h(v_k) \cdot h_3 \; ; \; k = 1, 2, 3,
\end{aligned}
\qquad \textbf{(4.10)}
$$

with the synaptic links;

$$
\begin{aligned}
I_{13}(t) &= \alpha \cdot [v_1(t) - v_{\text{rest}}] \; ; \\
I_{23}(t) &= \alpha \cdot [v_2(t) - v_{\text{rest}}] \; ; \\
I_{31}(t) &= \alpha \cdot [v_3(t) - v_{\text{rest}}] \; .
\end{aligned}
\qquad \textbf{(4.11)}
$$

Here we use our method of ‘back spread’ algorithmic goal: the real control signal is passing from the neuron 3 to the neuron 2, while the algorithmic definition of the goal follows the opposite direction, from 2 to 3, see Eqs.(4.14)-(4.15) below.

First, we apply SG algorithm Eq. (3.5) to the neuron 3;

$$I_{\text{control}}(t) = -\gamma \cdot [v_3(t) - v_{3*}(t)] \,. \tag{4.12}$$

The goal v3* of the tracking potential in the neuron 3 is defined as the inverse function to Eq. (4.2);

$$v_{3*}(t) = \frac{I_{31*}(t)}{\alpha} + v_{\text{rest}} \;. \tag{4.13}$$

The control current $I_{control}$ entering the neuron 3 is given also in the SG form Eq. (3.5);

$$I_{31*}(t) = -\gamma \cdot \Delta\big(I_{13}(t) - I_{23}(t)\big) \cdot [v_2(t) - v_{rest}] \,, \tag{4.14}$$

where Δ stands for the smooth model of delta-function;

$$\Delta(x) = \frac{1}{\sqrt{\pi} d} \exp\left\{-\frac{x^2}{d^2}\right\} \;;\; d = \text{const} > 0 \,. \tag{4.15}$$

The factor Δ in Eq. (4.14) switches on the control algorithm only for the synchronized currents I_{13} and I_{23}, and in the case of their time over-synchronization, i.e. only in the period of their epileptiform dynamics, leads the neuron 2 to the stabilization at the rest membrane potential.

This algorithm can be easily extended for a larger number of collective bursting neurons and their feedback links in the population.

For the numerical simulations that have shown below we have chosen these parameters I_{input1}=40, I_{input2}=42, α=10, γ=30, d=0.1.

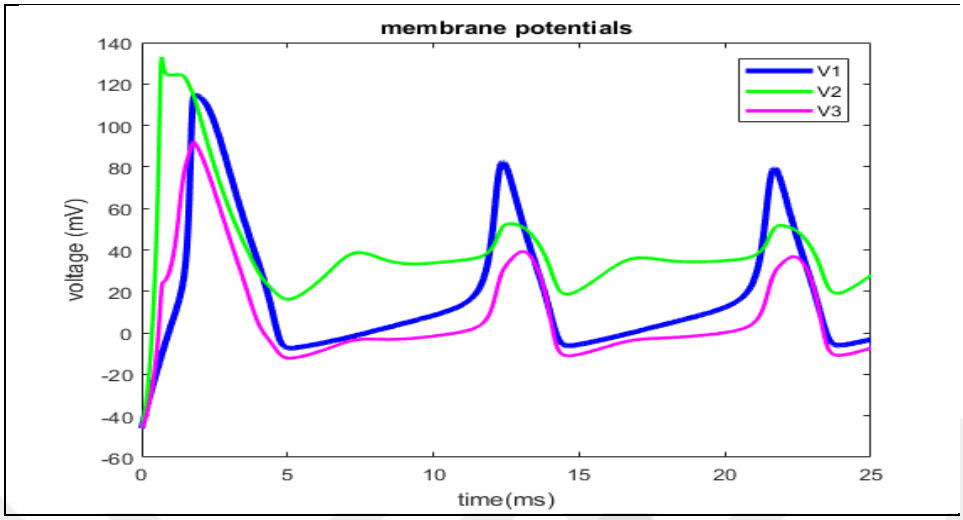

Figure 4.10: Neurons membrane potentials vs. time (membrane potential for first neuron v1– by blue color, for second neuron v2– by green color, for third neuron v3– by pink color)

On the Figure 4.10 one can see that after the beginning instability at the scale t=5 the potential v1 is suppressed around three times to compare with the bursting potential v2. This result seems to be great for such a basic control mechanism. Again collectively synchronized bursting was starting to increase (close to t=13 and t=23), the control model is switching on to drive the potential of the neuron 2 far away from the synchronization. The same is happen when t = 15 and t=24.

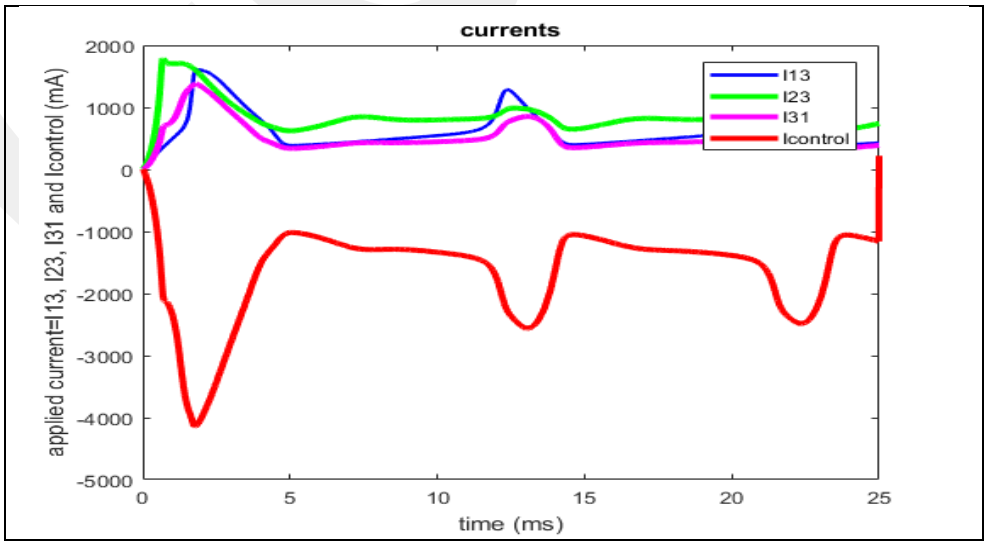

Figure 4.11: Currents vs. time (I_{13}– by blue color, I_{23}– by green color, I_{31}– by pink color)

Figure 4.11 demonstrate that $I_{control}$ was suppressed three times the currents. This control can give us good for a simple control system.

The supposed algorithm demonstrates only the primitive features of the bursting suppression. The simple control model Eqs. (4.14)-(4.15) needs to be sufficiently advanced for the better detecting the chaotic hyper-synchronization in the clusters and fasting more flexible details of the neuron dynamics.

4.4 Conclusions

The developed control algorithm [139] for tracking the membrane action potential of a single Hodgkin-Huxley neuron can be applied to a small structure of HH neuron showing epileptiform dynamics have basic features. In this population one of the neurons catch the over-synchronized neurons among its network neighbors and activates the feedback signal to some selected neurons in the population by removing epileptiform regime as a control element.

Chapter 5
Conclusions and Discussions

5.1 Basic statements of the thesis

1. Both algorithms, SG and TA, are successful for tracking goal potential in the HH neuron,
2. The choice of the plausible control depends on two basic criteria:
    - If the main factor is the minimization of the error *e(t)*, the target attractor is preferable.
    - If we consider performing the control by the minimum certain energy than the speed gradient has the priority.
3. For prolonged number of HH neurons in the networks, the error of tracking for the desired potential increase.
4. Two fundamental criteria for the evaluation of SG and TA algorithms are:
    - the error of tracking for the target potential,
    - the energy efficiency.

5.2 The set of main results

1. We modeled analytically and numerically (in MATLAB) the dynamical behavior of single and various chain structures of controlled Hodgkin-Huxley neurons.
2. Two alternative control algorithms have been successfully adopted for designing control external signal.
3. For the expanded number of HH neurons in the population MATLAB's calculation time is extremely increased for TA algorithm to compare with SG.
4. The transfer of control in the neural chain configuration needs more energy and larger control signal (current) as the chain is longer.
5. One control neuron in the population is able to suppress the over-synchronized epileptiform behavior in the small network with cumulative bursting and undesired oscillations in the HH neurons.

5.3 Perspectives of the research

In the small HH clusters one of the neurons performs a control tool for detecting and suppressing the hyper synchronization in the networks also it constructs and sends feedback signal driving to the resting membrane potential from collective bursting like epileptiform behavior. Thus, the approach developed in the thesis can provide crucial opportunities for the modeling such neuronal disorders as epilepsy, Alzheimer, Parkinson, paralysis, dementia and arrhythmia in large-scale neural networks. A number of neurons to be controlled in such networks is restricted by the amplitude of the control current and the energy consume required. In the perspective, our control algorithm could serve as a new model that designing a real-time electrical control system including a computer simulation tool and a neural prosthesis for the patients suffering from various nerve diseases. Therefore, this algorithm can be designed to work autonomously and detect a disorder in the real human brain.

5.4 Participation in the projects, conferences, publications

My study has been supported by TÜBİTAK (the Scientific and Technological Research Council of Turkey), Project no: 116F049, “Controlling Spiking and Bursting Dynamics in Hodgkin-Huxley Neurons” as master student scholarship for the period since November 2016 till January 2018.

The basic results of the thesis have been presented at the following conferences;

1. “Hızlı Gradyan Algoritması ile Hodgkin-Huxley Nöron Dinamikleri Kontrolü”, “II. Yaşam Bilimleri Kongresi”, in 23-25 February 2017, Abdullah Gül University, Kayseri / Turkey (the poster presentation).
2. “15th International Conference on Researches in Science and Technology (ICRST)”, in 23-24 June 2017, University of Malaya, Kuala Lumpur / Malaysia (oral presentation, the best presentation award).
3. “International conference on Theoretical and Applied Computer Science and Engineering-ICTACSE 2017” in 10-11 November 2017, Ankara University, Ankara / Turkey (oral presentation).

The basic results of the thesis research have been published in the following articles:

1. Borisenok, S., Ünal, Z. 2017. “Tracking of Arbitrary Regimes for Spiking and Bursting in the Hodgkin-Huxley Neuron”, MATTER: International Journal of Science and Technology, 3, 560-576, DOI: 10.20319/mijst.2017.32.560576.
2. Borisenok, S., Çatmabacak, Ö., Ünal, Z. 2018. “Control of Collective Bursting in Small Hodgkin-Huxley Neuron Clusters”, Commun.Fac.Sci.Univ.Ank.Series A2-A3, 60 (1), 21-30, DOI: 10.1501/commua1-2_0000000108.

BIBLIOGRAPHY

[1] "© 2014 WebMD, LLC. - Google'da Ara." [Online]. Available: https://www.google.com.tr/search?q=©+2014+WebMD%2C+LLC.&oq=©+2014+WebMD%2C+LLC.&aqs=chrome..69i57j33.5314j1j7&sourceid=chrome&ie=UTF-8. [Accessed: 27-Aug-2018].

[2] "© 2005 Pearson Prentice Hall Inc. neuron - Google'da Ara." [Online]. Available: https://www.google.com.tr/search?q=©+2005+Pearson+Prentice+Hall+Inc.+neuron&tbm=isch&tbs=rimg:CVZ0Se9vzsMtIjgia68YYL6uCbaEXJ5Uil3wxrxI_1Ln4t313HhV9Hr_12Gcnl5Y8ZcMhb_1E1W98ZMNlKAYszO6EK74CoSCSJrrxhgvq4JEe3Wx-IOIS6DKhIJtoRcnlSKXfAR8QL9kexCeGMqEgnGvEj8u. [Accessed: 31-Aug-2018].

[3] C. J. Lobb, Z. Chao, R. M. Fujimoto, and S. M. Potter, "Parallel event-driven neural network simulations using the Hodgkin-Huxley neuron model," *Proc. - Work. Princ. Adv. Distrib. Simulation, PADS*, pp. 16–25, 2005.

[4] R. Siciliano, "The Hodgkin-Huxley model - Its extensions , analysis and numerics.," p. 41, 2012.

[5] Y. Timofeeva, "Lecture Notes_Single neuron models.," pp. 1–12, 2008.

[6] C. D. Brody and J. J. Hopfield, "Simple Networks for Spike-Timing-Based Computation, with Application to Olfactory Processing," *Neuron*, vol. 37, no. 5, pp. 843–852, Mar. 2003.

[7] J. M. Bower, Ed., *20 Years of Computational Neuroscience*. New York, NY: Springer New York, 2013.

[8] M. H. A. Awadalla and M. Abdellatif Sadek, "Spiking neural network-based control chart pattern recognition," *Alexandria Eng. J.*, vol. 51, no. 1, pp. 27–35, Mar. 2012.

[9] M. I. Rabinovich and H. D. I. Abarbanel, "THE ROLE OF CHAOS IN NEURAL SYSTEMS," 1998.

[10] N. Purali, "Firing Properties of the Soma and Axon of the Abdominal Stretch Receptor Neurons in the Crayfish (Astacus leptodactylus)," 2002.

[11] P. M. DiLorenzo and J. D. (Jonathan D. . Victor, *Spike timing : mechanisms and function*. Taylor & Francis/CRC Press, 2013.

[12] S. H. Strogatz and I. Stewart, "Coupled oscillators and biological

synchronization.,” *Sci. Am.*, vol. 269, no. 6, pp. 102–9, Dec. 1993.

[13] G. S. Cymbalyuk, R. L. Calabrese, and A. L. Shilnikov, “How a neuron model can demonstrate co-existence of tonic spiking and bursting,” *Neurocomputing*, vol. 65–66, pp. 869–875, Jun. 2005.

[14] L. F. Abbott, E. Marder, and S. L. Hooper, “Communicated by Allen Selverston Oscillating Networks: Control of Burst Duration by Electrically Coupled Neurons,” 1991.

[15] R. C. Elson, R. Huerta, H. D. I. Abarbanel, M. I. Rabinovich, and A. I. Selverston, “Dynamic Control of Irregular Bursting in an Identified Neuron of an Oscillatory Circuit,” *J. Neurophysiol.*, vol. 82, no. 1, pp. 115–122, Jul. 1999.

[16] G. Drion *et al.*, “M-type channels selectively control bursting in rat dopaminergic neurons.,” *Eur. J. Neurosci.*, vol. 31, no. 5, pp. 827–35, Mar. 2010.

[17] D. Jaeger, “The Control of Spiking by Synaptic Input in Striatal and Pallidal Neurons,” Springer, Boston, MA, 2002, pp. 209–216.

[18] J. E. Lewis, B. Lindner, B. Laliberté, and S. Groothuis, “Control of neuronal firing by dynamic parallel fiber feedback: implications for electrosensory reafference suppression.,” *J. Exp. Biol.*, vol. 210, no. Pt 24, pp. 4437–47, Dec. 2007.

[19] C. Meisel, A. Klaus, C. Kuehn, and D. Plenz, “Critical Slowing Down Governs the Transition to Neuron Spiking,” *PLOS Comput. Biol.*, vol. 11, no. 2, p. e1004097, Feb. 2015.

[20] J. Cardin, M. Carlén, K. Meletis, U. Knoblich, F. Z.- Nature, and undefined 2009, “Driving fast-spiking cells induces gamma rhythm and controls sensory responses,” *nature.com*.

[21] A. Sucapane, G. Cellot, … M. P.-J. of, and undefined 2009, “Interactions between cultured neurons and carbon nanotubes: a nanoneuroscience vignette,” *ingentaconnect.com*.

[22] Z. Yu, T. McKnight, M. Ericson, … A. M.-, B. and Medicine, and undefined 2012, “Vertically aligned carbon nanofiber as nano-neuron interface for monitoring neural function,” *Elsevier*.

[23] E. J. Tehovnik, A. S. Tolias, F. Sultan, W. M. Slocum, and N. K. Logothetis, “Direct and Indirect Activation of Cortical Neurons by Electrical Microstimulation,” *J. Neurophysiol.*, vol. 96, no. 2, pp. 512–521, Aug. 2006.

[24] A. Fradkov, “Cybernetical physics: from control of chaos to quantum control,”

2007.

[25] A. A. Kolesnikov, “Introduction of synergetic control,” *Proc. Am. Control Conf.*, pp. 3013–3016, 2014.

[26] A. L. HODGKIN and A. F. HUXLEY, “A quantitative description of membrane current and its application to conduction and excitation in nerve.,” *J. Physiol.*, vol. 117, no. 4, pp. 500–44, Aug. 1952.

[27] T. R. CHAY, Y. S. FAN, and Y. S. LEE, “BURSTING, SPIKING, CHAOS, FRACTALS, AND UNIVERSALITY IN BIOLOGICAL RHYTHMS,” *Int. J. Bifurc. Chaos*, vol. 05, no. 03, pp. 595–635, Jun. 1995.

[28] Y. Ji and Y. W. Wang, “Bursting behavior in the piece-wise linear planar neuron model with periodic stimulation,” *Chinese Phys. Lett.*, vol. 32, no. 4, 2015.

[29] S. Borisenok, “Speed Gradient Driving of Neuron Spiking.” 2015.

[30] STROGARTZ and S. H., “Nonlinear Dynamics and Chaos : With Applications to Physics, Biology,” *Chem. Eng.*, vol. 441, 1994.

[31] R. FitzHugh, “Mathematical models of threshold phenomena in the nerve membrane,” *Bull. Math. Biophys.*, vol. 17, no. 4, pp. 257–278, Dec. 1955.

[32] J. Nagumo, S. Arimoto, and S. Yoshizawa, “An Active Pulse Transmission Line Simulating Nerve Axon*,” *Proc. IRE*, vol. 50, no. 10, pp. 2061–2070, 1962.

[33] Eugene M.Izhikevich, “Resonate-and-fire neurons,” *Neural Networks*, vol. 14, no. 6–7, pp. 883–894, Jul. 2001.

[34] E. M. Izhikevich, “Simple model of spiking neurons,” *IEEE Trans. Neural Networks*, vol. 14, no. 6, pp. 1569–1572, Nov. 2003.

[35] J. Touboul and R. Brette, “Spiking Dynamics of Bidimensional Integrate-and-Fire Neurons,” *SIAM J. Appl. Dyn. Syst.*, vol. 8, no. 4, pp. 1462–1506, Jan. 2009.

[36] S. Visser and S. A. Van Gils, “Lumping Izhikevich neurons,” *EPJ Nonlinear Biomed. Phys.*, vol. 2, no. 1, p. 6, Dec. 2014.

[37] “On the interspike-intervals of periodically-driven integrate-and-fire models,” *J. Math. Anal. Appl.*, vol. 423, no. 1, pp. 456–479, Mar. 2015.

[38] G. Teschl, “Ordinary Differential Equations and Dynamical Systems - Gerald Teschl - Google Kitaplar,” 2012. [Online]. Available: https://books.google.com.tr/books?hl=tr&lr=&id=FZ0CAQAAQBAJ&oi=fnd&pg=PR9&dq=Teschl+2012&ots=YkNb1Nbpa5&sig=hH0fGttuyqOKJG6b41s_1Ggf5Uc&redir_esc=y#v=onepage&q=Teschl 2012&f=false. [Accessed: 30-Aug-2018].

[39] E. Izhikevich and R. FitzHugh, “FitzHugh-Nagumo model,” *Scholarpedia*, vol. 1, no. 9, p. 1349, 2006.

[40] R. FitzHugh, “Impulses and Physiological States in Theoretical Models of Nerve Membrane,” *Biophys. J.*, vol. 1, no. 6, pp. 445–466, 1961.

[41] K. P. Hadeler, U. an der Heiden, and K. Schumacher, “Generation of the nervous impulse and periodic oscillations,” *Biol. Cybern.*, vol. 23, no. 4, pp. 211–218, Dec. 1976.

[42] T. Nomura and Y. Asai, *BOOK : Computational Electrophysiology. Dynamical Systems and Bifurcations*. 2011.

[43] S. Vaidyanathan, “Adaptive control of the FitzHugh-Nagumo chaotic neuron model,” *Int. J. PharmTech Res.*, vol. 8, no. 6, pp. 117–127, 2015.

[44] J. Hindmarsh, R. R.-P. R. S. L. B, and undefined 1984, “A model of neuronal bursting using three coupled first order differential equations,” *rspb.royalsocietypublishing.org*.

[45] “Probabilistic neural networks,” *Neural Networks*, vol. 3, no. 1, pp. 109–118, Jan. 1990.

[46] F. Beck, “Synaptic Quantum Tunnelling in Brain Activity,” *NeuroQuantology*, vol. 6, no. 2, Jun. 2008.

[47] A. Pechen and S. Borisenok, “Energy Transfer in Two-Level Quantum Systems via Speed Gradient-Based Algorithm,” *IFAC-PapersOnLine*, vol. 48, no. 11, pp. 446–450, Jan. 2015.

[48] V. Z.-M. hypotheses and undefined 1994, “Bioelectric signals in neuron structures and the Josephson effect,” *Elsevier*.

[49] P. Crotty, D. Schult, and K. Segall, “Josephson junction simulation of neurons,” *Phys. Rev. E*, vol. 82, no. 1, p. 011914, Jul. 2010.

[50] K. Segall, S. Guo, P. Crotty, D. Schult, M. M.-P. B. C. Matter, and undefined 2014, “Phase-flip bifurcation in a coupled Josephson junction neuron system,” *Elsevier*.

[51] S. Borisenok, A. Fradkov, and A. Proskurnikov, “Speed gradient control of qubit state.”

[52] A. Hodgkin, A. Huxley, B. K.-T. J. of physiology, and undefined 1952, “Measurement of current-voltage relations in the membrane of the giant axon of Loligo,” *Wiley Online Libr.*

[53] A. L. Hodgkin and A. F. Huxley, “The dual effect of membrane potential on

sodium conductance in the giant axon of *Loligo*," *J. Physiol.*, vol. 116, no. 4, pp. 497–506, Apr. 1952.

[54] A. L. Hodgkin and A. F. Huxley, "The Components of Membrane Conductance in the Giant Axon of Lolıgo," pp. 473–496, 1952.

[55] A. L. Hodgkin and A. F. Huxley, "Currents carried by sodium and potassium ions through the membrane of the giant axon of *Loligo*," *J. Physiol.*, vol. 116, no. 4, pp. 449–472, Apr. 1952.

[56] J. Rinzel, "Dicussion: Electrical excitability of cells, theory and experiment: Rview of the Hodkin-Huxley foundation and an update," *Bull. Math. Biol.*, vol. 52, no. 1/2, pp. 5–23, 1990.

[57] S. Doi, J. Inoue, and Z. Pan, "Computational Electrophysiology," no. 1952, 2010.

[58] K. Cole, A. H.-T. J. of general physiology, and undefined 1939, "Membrane and protoplasm resistance in the squid giant axon," *jgp.rupress.org*.

[59] M. Nelson and J. Rinzel, "The Hodgkin-Huxley Model," *Genesis*, vol. 125, no. 20, pp. 29–50, 1990.

[60] D. Purves, "Neuroscience, 3rd Edition."

[61] H. J. Curtis and K. S. Cole, "Membrane action potentials from the squid giant axon," *J. Cell. Comp. Physiol.*, vol. 15, no. 2, pp. 147–157, Apr. 1940.

[62] A. L. HODGKIN and A. F. HUXLEY, "Action Potentials Recorded from Inside a Nerve Fibre," *Nat. 1939 1443651*, vol. 144, no. 3651, p. 710, Oct. 1939.

[63] J. B.-A. für die gesamte P. des M. und and undefined 1902, "Untersuchungen zur Thermodynamik der bioelektrischen Ströme," *Springer*.

[64] G. Marmont, "Studies on the axon membrane. I. A new method," *J. Cell. Comp. Physiol.*, vol. 34, no. 3, pp. 351–382, Dec. 1949.

[65] K. S. Cole, "Some Physical Aspects of Bioelectric Phenomena," *Proc. Natl. Acad. Sci.*, vol. 35, no. 10, pp. 558–566, Oct. 1949.

[66] M. Diehl, "Modelling Hodgkin-Huxley," *Model. Mol. Biotechnol.*, no. 2170370, p. 22, 2004.

[67] J. Malmivuo and R. Plonsey, "Bioelectromagnetism: Principles and Applications of Bioelectric and ... - Professor of Bioelectromagnetism and Head of the Ragnar Granit Institute Jaakko Malmivuo, Jaakko Malmivuo, Robert Plonsey, Professor of Biomedical Engineering Robert Plonsey - Google Kitaplar," 1995. [Online]. Available: https://books.google.com.tr/books?hl=tr&lr=&id=H9CFM0TqWwsC&oi=fnd&p

g=PR15&dq=bioelectromagnetism+Active+Behavior+of+the+Cell+Membrane&ots=pAsrOjAaUR&sig=kw7XZUAycNTWKW89s9q7PhF3HIw&redir_esc=y#v=onepage&q&f=false. [Accessed: 30-Aug-2018].

[68] K. S. (Kenneth S. Cole, *Membranes, ions, and impulses : a chapter of classical biophysics*. University of California Press, 1972.

[69] E. Agi, C. Ozgen, and N. Purali, "Modeling of Gate Control Neuronal Circuitry Including Morphologies and Physiologies of Component Neurons and Fibres."

[70] J. Guckenheimer and R. A. Oliva, "Chaos in the Hodgkin--Huxley Model," *SIAM J. Appl. Dyn. Syst.*, vol. 1, no. 1, pp. 105–114, Jan. 2002.

[71] T.-L. Horng and M.-W. Huang, "Spontaneous Oscillations in Hodgkin-Huxley Model."

[72] J. Wang, L. Chen, and X. Fei, "Analysis and control of the bifurcation of Hodgkin-Huxley model," *Chaos, Solitons and Fractals*, vol. 31, no. 1, pp. 247–256, 2007.

[73] A. B. Neiman, K. Dierkes, B. Lindner, L. Han, and A. L. Shilnikov, "Spontaneous voltage oscillations and response dynamics of a Hodgkin-Huxley type model of sensory hair cells," *J. Math. Neurosci.*, vol. 1, no. 1, p. 11, 2011.

[74] F. Hoppensteadt, "Heuristics for the Hodgkin-Huxley system," *Math. Biosci.*, vol. 245, no. 1, pp. 56–60, 2013.

[75] A. Tonnelier, "Categorization of Neural Excitability Using Threshold Models," *Neural Comput.*, vol. 17, no. 7, pp. 1447–1455, Jul. 2005.

[76] E. Yilmaz and M. Ozer, "Collective firing regularity of a scale-free Hodgkin–Huxley neuronal network in response to a subthreshold signal," *Phys. Lett. A*, vol. 377, no. 18, pp. 1301–1307, Aug. 2013.

[77] T. Kitajima and Z. Feng, "Subthreshold Resonance Oscillation and Generation of Action Potential," 2014.

[78] "Mathematical Biosciences Institute :: Workshop 1: Control and Modulation of Neuronal and Motor Systems." [Online]. Available: https://mbi.osu.edu/event/?id=1062. [Accessed: 31-Aug-2018].

[79] S. J. Schiff, "Neural Control Engineering: The Emerging Intersection Between Control Theory ... - Steven J. Schiff - Google Kitaplar," 2012. [Online]. Available: https://books.google.com.tr/books?hl=tr&lr=&id=P9UvTQtnqKwC&oi=fnd&pg=PR7&dq=Schiff,+2012+control+single+neuron&ots=hC8YWAS5Wl&sig=S6F

s__bbJIWXn9NU_CtUktwYIog&redir_esc=y#v=onepage&q=Schiff%2C 2012 control single neuron&f=false. [Accessed: 31-Aug-2018].

[80] I. Dasanayake and J.-S. Li, "Optimal design of minimum-power stimuli for phase models of neuron oscillators," *Phys. Rev. E*, vol. 83, no. 6, p. 061916, Jun. 2011.

[81] Y. Ahmadian, A. M. Packer, R. Yuste, and L. Paninski, "Designing optimal stimuli to control neuronal spike timing.," *J. Neurophysiol.*, vol. 106, no. 2, pp. 1038–53, Aug. 2011.

[82] P. Danzl, J. Hespanha, and J. Moehlis, "Event-based minimum-time control of oscillatory neuron models," *Biol. Cybern.*, vol. 101, no. 5–6, pp. 387–399, Dec. 2009.

[83] S. Ching and J. T. Ritt, "Control strategies for underactuated neural ensembles driven by optogenetic stimulation," *Front. Neural Circuits*, vol. 7, p. 54, Apr. 2013.

[84] J. Liu, K. G. Oweiss, and H. K. Khalil, "Feedback control of the spatiotemporal firing patterns of neural microcircuits," in *49th IEEE Conference on Decision and Control (CDC)*, 2010, pp. 4679–4684.

[85] S. J. Schiff and T. Sauer, "Kalman filter control of a model of spatiotemporal cortical dynamics," *BMC Neurosci.*, vol. 9, no. Suppl 1, p. O1, Jul. 2008.

[86] Li, "Adaptive Inverse Control of Neural Spatiotemporal Spike Patterns With a Reproducing Kernel Hilbert Space (RKHS) Framework," *IEEE Trans. Neural Syst. Rehabil. Eng.*, vol. 21, no. 4, pp. 532–543, Jul. 2013.

[87] T. Kano and S. Kinoshita, "Control of individual phase relationship between coupled oscillators using multilinear feedback," *Phys. Rev. E*, vol. 81, no. 2, p. 026206, Feb. 2010.

[88] P. J. Uhlhaas and W. Singer, "Neural Synchrony in Brain Disorders: Relevance for Cognitive Dysfunctions and Pathophysiology," *Neuron*, vol. 52, no. 1, pp. 155–168, Oct. 2006.

[89] V. S. Sohal, F. Zhang, O. Yizhar, and K. Deisseroth, "Parvalbumin neurons and gamma rhythms enhance cortical circuit performance," *Nature*, vol. 459, no. 7247, pp. 698–702, Jun. 2009.

[90] A. Witt, A. Palmigiano, A. Neef, A. El Hady, F. Wolf, and D. Battaglia, "Controlling the oscillation phase through precisely timed closed-loop optogenetic stimulation: a computational study," *Front. Neural Circuits*, vol. 7, p. 49, Apr. 2013.

[91] L. Grosenick, J. H. Marshel, and K. Deisseroth, “Closed-Loop and Activity-Guided Optogenetic Control,” *Neuron*, vol. 86, no. 1, pp. 106–139, Apr. 2015.

[92] A. Nabi and J. Moehlis, “Single input optimal control for globally coupled neuron networks,” *J. Neural Eng.*, vol. 8, no. 6, p. 065008, Oct. 2011.

[93] E. Schöll, G. Hiller, P. Hövel, and M. A. Dahlem, “Time-delayed feedback in neurosystems.,” *Philos. Trans. A. Math. Phys. Eng. Sci.*, vol. 367, no. 1891, pp. 1079–96, Mar. 2009.

[94] A. Nabi and J. Moehlis, “Nonlinear hybrid control of phase models for coupled oscillators,” in *Proceedings of the 2010 American Control Conference*, 2010, pp. 922–923.

[95] S. J. Schiff, K. Jerger, D. H. Duong, T. Chang, M. L. Spano, and W. L. Ditto, “Controlling chaos in the brain,” *Nature*, vol. 370, no. 6491, pp. 615–620, Aug. 1994.

[96] J. Moehlis, E. Shea-Brown, and H. Rabitz, “Optimal Inputs for Phase Models of Spiking Neurons,” *J. Comput. Nonlinear Dyn.*, vol. 1, no. 4, p. 358, Oct. 2006.

[97] P. Danzl, A. Nabi, and J. Moehlis, “CHARGE-BALANCED SPIKE TIMING CONTROL FOR PHASE MODELS OF SPIKING NEURONS,” vol. 28, no. 4, pp. 1413–1435, 2010.

[98] A. Nabi and J. Moehlis, “Charge-Balanced Optimal Inputs for Phase Models of Spiking Neurons,” in *ASME 2009 Dynamic Systems and Control Conference, Volume 1*, 2009, pp. 685–687.

[99] T. Stigen, P. Danzl, J. Moehlis, and T. Netoff, “Controlling spike timing and synchrony in oscillatory neurons,” *BMC Neurosci.*, vol. 12, no. Suppl 1, p. P223, Jul. 2011.

[100] A. Nabi and J. Moehlis, “Time optimal control of spiking neurons,” *J. Math. Biol.*, vol. 64, no. 6, pp. 981–1004, May 2012.

[101] A. Nabi, M. Mirzadeh, F. Gibou, and J. Moehlis, “Minimum energy desynchronizing control for coupled neurons,” *J. Comput. Neurosci.*, vol. 34, no. 2, pp. 259–271, Apr. 2013.

[102] R. Jolivet, T. J., and W. Gerstner, “The Spike Response Model: A Framework to Predict Neuronal Spike Trains,” Springer, Berlin, Heidelberg, 2003, pp. 846–853.

[103] B.-S. Chen and C.-W. Li, “Robust Observer-Based Tracking Control of Hodgkin-Huxley Neuron Systems Under Environmental Disturbances,” *Neural Comput.*, vol. 22, no. 12, pp. 3143–3178, Dec. 2010.

[104] Y.-T. Chang and B.-S. Chen, “A Fuzzy Approach for Robust Reference-Tracking-Control Design of Nonlinear Distributed Parameter Time-Delayed Systems and Its Application,” *IEEE Trans. Fuzzy Syst.*, vol. 18, no. 6, pp. 1041–1057, Dec. 2010.

[105] S. H. Strogatz, “Nonlinear Dynamics and Chaos : With Applications to Physics, Biology, Chemistry, and Engineering,” May 2018.

[106] J. C. A. de Pontes, R. L. Viana, S. R. Lopes, C. A. S. Batista, and A. M. Batista, “Bursting synchronization in non-locally coupled maps,” *Phys. A Stat. Mech. its Appl.*, vol. 387, no. 16–17, pp. 4417–4428, Jul. 2008.

[107] S. Coombes and P. C. Bressloff, “Erratum: Mode locking and Arnold tongues in integrate-and-fire neural oscillators [Phys. Rev. E **60** , 2086 (1999)],” *Phys. Rev. E*, vol. 63, no. 5, p. 059901, Apr. 2001.

[108] M. Christen, R. Stoop, J. Buchli, and M. Christen, “Phase and frequency locking in detailed neuron models Towards biological hearing aids View project Mapping Human Values: Text-mining Obituaries for Networks of Virtues, Values, and Constituents of Wellbeing View project Ruedi Stoop ETH Zurich Phase and frequency locking in detailed neuron models.”

[109] S. A. Campbell, “Time Delays in Neural Systems,” Springer, Berlin, Heidelberg, 2007, pp. 65–90.

[110] S. Coombes, R. Thul, and K. C. A. Wedgwood, “Nonsmooth dynamics in spiking neuron models,” *Phys. D Nonlinear Phenom.*, vol. 241, no. 22, pp. 2042–2057, Nov. 2012.

[111] Y. G. Zheng and Z. H. Wang, “Time-delay effect on the bursting of the synchronized state of coupled Hindmarsh-Rose neurons,” *Chaos An Interdiscip. J. Nonlinear Sci.*, vol. 22, no. 4, p. 043127, Dec. 2012.

[112] A. PANCHUK, D. P. ROSIN, P. HÖVEL, and E. SCHÖLL, “SYNCHRONIZATION OF COUPLED NEURAL OSCILLATORS WITH HETEROGENEOUS DELAYS,” *Int. J. Bifurc. Chaos*, vol. 23, no. 12, p. 1330039, Dec. 2013.

[113] N. Vasović, N. Burić, K. Todorović, and I. Grozdanović, “Synchronization of the minimal models of bursting neurons coupled by delayed chemical or electrical synapses,” *Chinese Phys. B*, vol. 21, no. 1, p. 010203, Jan. 2012.

[114] M. Mamat, P. W. Kurniawan, A. Kartono, M. Mamat, P. W. Kurniawan, and A. Kartono, “Development of Dynamics and Synchronization Model for Coupled

Neurons Using Hindmarsh-Rose Model," 2013.

[115] J. Wang, T. Zhang, and Y. Che, "Chaos control and synchronization of two neurons exposed to ELF external electric field," *Chaos, Solitons & Fractals*, vol. 34, no. 3, pp. 839–850, Nov. 2007.

[116] H. Yu, J. Wang, C. Liu, B. Deng, and X. Wei, "Delay-induced synchronization transitions in small-world neuronal networks with hybrid electrical and chemical synapses," *Phys. A Stat. Mech. its Appl.*, vol. 392, no. 21, pp. 5473–5480, Nov. 2013.

[117] S. Plotnikov, J. Lehnert, A. Fradkov, and E. Schöll, "CONTROL OF SYNCHRONIZATION IN DELAY-COUPLED NEURAL HETEROGENEOUS NETWORKS."

[118] S. Coombes and C. Laing, "Delays in activity-based neural networks.," *Philos. Trans. A. Math. Phys. Eng. Sci.*, vol. 367, no. 1891, pp. 1117–29, Mar. 2009.

[119] C. Liu *et al.*, "The effects of time delay on the stochastic resonance in feed-forward-loop neuronal network motifs," *Commun. Nonlinear Sci. Numer. Simul.*, vol. 19, no. 4, pp. 1088–1096, Apr. 2014.

[120] P. Perlikowski, S. Yanchuk, O. V. Popovych, and P. A. Tass, "Periodic patterns in a ring of delay-coupled oscillators," *Phys. Rev. E*, vol. 82, no. 3, p. 036208, Sep. 2010.

[121] A. Ş. Demirkol and S. Özoğuz, "İstanbul Ticaret Üniversitesi Fen Bilimleri Dergisi Yıl: 12 Sayı: 24 Güz," 2013.

[122] P. J. Neefs, H. J. C. Huijberts, and H. Nijmeijer, "On Time-Delayed Coupled Hindmarsh-Rose Neurons: Stability of Equilibria and Synchronisation," 2008.

[123] I. Franović, K. Todorović, N. Vasović, and N. Burić, "Stability, bifurcations, and dynamics of global variables of a system of bursting neurons," *Chaos An Interdiscip. J. Nonlinear Sci.*, vol. 21, no. 3, p. 033109, Sep. 2011.

[124] N. Serap Sengor, "Model of Medium Spiny Neurons and Synchronization by Dopamine Level," 2014.

[125] B. M. Adhikari, A. Prasad, and M. Dhamala, "Time-delay-induced phase-transition to synchrony in coupled bursting neurons," *Chaos An Interdiscip. J. Nonlinear Sci.*, vol. 21, no. 2, p. 023116, Jun. 2011.

[126] C. A. S. Batista, R. L. Viana, F. A. S. Ferrari, S. R. Lopes, A. M. Batista, and J. C. P. Coninck, "Control of bursting synchronization in networks of Hodgkin-Huxley-type neurons with chemical synapses," *Phys. Rev. E*, vol. 87, no. 4, p.

042713, Apr. 2013.

[127] F. Fröhlich and S. Jezernik, “Feedback control of Hodgkin–Huxley nerve cell dynamics,” *Control Eng. Pract.*, vol. 13, no. 9, pp. 1195–1206, Sep. 2005.

[128] G. Ullah and S. J. Schiff, “Tracking and control of neuronal Hodgkin-Huxley dynamics,” *Phys. Rev. E*, vol. 79, no. 4, p. 040901, Apr. 2009.

[129] L. Ding and C. Hou, “Stabilizing control of Hopf bifurcation in the Hodgkin-Huxley model via washout filter with linear control term,” *Nonlinear Dyn.*, vol. 60, no. 1–2, pp. 131–139, 2010.

[130] R. Ö. Türkiye Bilimsel ve Teknik Araştırma Kurumu. and Elektrik Mühendisleri Odası (Turkey), *Elektrik : Turkish journal of electrical engineering & computer sciences.*, vol. 18, no. 4. Scientific and Technical Research Council of Turkey (TÜBİTAK) and Chamber of Electrical Engineers (EMO-TMMOB), 2010.

[131] A. L. Fradkov and A. A. Stotsky, “Speed gradient adaptive control algorithms for mechanical systems,” *Int. J. Adapt. Control Signal Process.*, vol. 6, no. 3, pp. 211–220, May 1992.

[132] A. L. Fradkov and A. Y. Pogromsky, “Speed gradient control of chaotic continuous-time systems,” *IEEE Trans. Circuits Syst. I Fundam. Theory Appl.*, vol. 43, no. 11, pp. 907–913, 1996.

[133] A. L. (Aleksandr L. Fradkov, I. V. (Il′ia V. Miroshnik, and V. O. Nikiforov, *Nonlinear and adaptive control of complex systems*. .

[134] A. A. Selivanov, J. Lehnert, T. Dahms, P. Hövel, A. L. Fradkov, and E. Schöll, “Adaptive synchronization in delay-coupled networks of Stuart-Landau oscillators,” *Phys. Rev. E*, vol. 85, no. 1, p. 016201, Jan. 2012.

[135] A. L. Fradkov and A. Y. Pogromsky, *Introduction to Control of Oscillations and Chaos*, vol. 35. WORLD SCIENTIFIC, 1998.

[136] A. L. Fradkov, “Cybernetical Physics: From Control of Chaos to Quantum Control - A. Fradkov - Google Kitaplar,” 2007. [Online]. Available: https://books.google.com.tr/books?hl=tr&lr=&id=nE4boHiXtjYC&oi=fnd&pg=PA1&dq=Fradkov,+A.L.,+Cybernetical+physics:+From+control+of+chaos+to+quantum+control,+Springer,+Berlin,+2007.&ots=VY--gYRZmW&sig=DZJltQcRoNFyTynasMEcxhiFJqY&redir_esc=y#v=onepage&q=Frad. [Accessed: 31-Aug-2018].

[137] C. H. Skiadas and I. Dimotikalis, “Chaotic Systems: Theory and Applications -

Christos H. Skiadas, Ioannis Dimotikalis - Google Kitaplar," 2009. [Online]. Available: https://books.google.com.tr/books?hl=tr&lr=&id=p_FpDQAAQBAJ&oi=fnd&pg=PR5&dq=Chaotic+Systems:+Theory+and+Applications&ots=QjikrtSCFn&sig=Z8ZukCzn7tQyB4m8YTHqXMOo4D8&redir_esc=y#v=onepage&q=Chaotic Systems%3A Theory and Applications&f=false. [Accessed: 31-Aug-2018].

[138] A. A. Kolesnikov, "Introduction of synergetic control," in *2014 American Control Conference*, 2014, pp. 3013–3016.

[139] S. Borisenok and Z. Ünal, "Date of Publication: 10 th," *Int. J. Sci. Technol.*, vol. 3, pp. 560–576, 2017.

[140] R. Carter, "The Human Brain Book | Rita Carter | download," 2014. [Online]. Available: http://b-ok.xyz/book/2739212/cdcd64. [Accessed: 31-Aug-2018].

[141] G. Petkov, M. Goodfellow, M. P. Richardson, and J. R. Terry, "A Critical Role for Network Structure in Seizure Onset: A Computational Modeling Approach," *Front. Neurol.*, vol. 5, p. 261, Dec. 2014.

[142] M. Lopez-Rodriguez and G. Hamilton, "Editorial," *Cent. Nerv. Syst. Agents Med. Chem.*, vol. 10, no. 1, pp. 1–2, Mar. 2010.

[143] S. Naze, "Multiscale Computational Modeling of Epileptic Seizures : from macro to microscopic dynamics," *http://www.theses.fr*, May 2015.

[144] F. Wendling, P. Benquet, F. Bartolomei, and V. Jirsa, "Computational models of epileptiform activity," *J. Neurosci. Methods*, vol. 260, pp. 233–251, Feb. 2016.

[145] S. B. O. R. I. Senok, Ö. Çatmabacak, and Z. Ünal, "CONTROL OF COLLECTIVE BURSTING IN SMALL HODGKIN- HUXLEY NEURON CLUSTERS," 2018, vol. 60, no. 1, pp. 21–30.